AD-A151 286 THE BEHAVIOR OF THE ATMOSPHERE IN THE DESERT PLANETARY BOUNDARY LAYER(U) BEN-GURION UNIV OF THE NEGEV SEDE BOQER (ISRAEL) JACOB BLAUST.. L BERKOFSKY 14 OCT 84 1/1

UNCLASSIFIED AFOSR-TR-85-0227 AFOSR-84-0036 F/G 4/1 NL

END

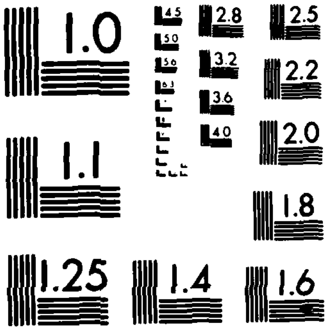

MICROCOPY RESOLUTION TEST CHART
NATIONAL BUREAU OF STANDARDS-1963-A

AFOSR-TR- 85-0227

AD-A151 286

FINAL REPORT

LOUIS BERKOFSKY

THE BEHAVIOR OF THE ATMOSPHERE IN THE DESERT PLANETARY BOUNDARY LAYER

AFOSR-84-0036

THE JACOB BLAUSTEIN INSTITUTE FOR DESERT RESEARCH
BEN-GURION UNIVERSITY OF THE NEGEV
SEDE BOQER CAMPUS 84990, ISRAEL

15 OCTOBER 1983 - 14 OCTOBER 1984

85 02 27 037

UNCLASSIFIED
SECURITY CLASSIFICATION OF THIS PAGE (When Data Entered)

REPORT DOCUMENTATION PAGE

READ INSTRUCTIONS BEFORE COMPLETING FORM

1. REPORT NUMBER: AFOSR-TR- 85-0227	2. GOVT ACCESSION NO.: AD A151256
3. RECIPIENT'S CATALOG NUMBER	
4. TITLE (and Subtitle): THE BEHAVIOR OF THE ATMOSPHERE IN THE DESERT PLANETARY BOUNDARY LAYER.	5. TYPE OF REPORT & PERIOD COVERED: Final Scientific Report 15 October 1983-14 October 1984
	6. PERFORMING ORG. REPORT NUMBER
7. AUTHOR(s): Louis Berkofsky	8. CONTRACT OR GRANT NUMBER(s): AFOSR-84-0036
9. PERFORMING ORGANIZATION NAME AND ADDRESS: The Jacob Blaustein Institute for Desert Research, Ben-Gurion University of the Negev, Sede Boqer Campus 84990, Israel	10. PROGRAM ELEMENT, PROJECT, TASK AREA & WORK UNIT NUMBERS: 61102F 2310/A1
11. CONTROLLING OFFICE NAME AND ADDRESS: U.S. Air Force Office of Scientific Research/NC, Bolling AFB, D.C. 20332-6448	12. REPORT DATE: 14 October 1984
	13. NUMBER OF PAGES: 81
14. MONITORING AGENCY NAME & ADDRESS(if different from Controlling Office)	15. SECURITY CLASS. (of this report): Unclassified
	15a. DECLASSIFICATION/DOWNGRADING SCHEDULE

16. DISTRIBUTION STATEMENT (of this Report)

Approved for public release, distribution unlimited

17. DISTRIBUTION STATEMENT (of the abstract entered in Block 20, if different from Report)

18. SUPPLEMENTARY NOTES

19. KEY WORDS (Continue on reverse side if necessary and identify by block number)

Atmosphere, Desert, Boundary Layer, Numerical Model, Inversion, Transport, Mesoscale, Dust, Limited Area Model

20. ABSTRACT (Continue on reverse side if necessary and identify by block number)

One of the aims of this investigation was to develop a limited area planetary boundary layer desert model for computers of limited power. We derived a general system of vertically integrated equations, including a dust concentration equation and an inversion height equation. The boundary layer was divided into a constant flux layer, a transition layer, and an inversion layer. The model equations predict the mean (vertically averaged) winds in the transition layer, the potential temperature at the top of the

DD FORM 1 JAN 73 1473 EDITION OF 1 NOV 65 IS OBSOLETE

UNCLASSIFIED
SECURITY CLASSIFICATION OF THIS PAGE (When Data Entered)

85 02 27 037

surface layer, the potential temperature at the ground, the height of the inversion layer, the dust concentration at the top of the surface layer, the moisture at the top of the surface layer, and the soil moisture at the ground. The radiation flux is also calculated as a function of time.

The equations were programmed for solution on a 300 x 600 km grid, with 10 km grid spacing, on a grid staggered in both time and space. The lateral boundary conditions were of the radiation type.

Initially, the one-dimensional version was tested (no horizontal advection). All fields showed reasonable evolution for a twenty-four hour prediction. Data (dust concentration, inversion height) are now being gathered for verification.

The two-dimensional version was first run with a time step of two minutes and boundary conditions held fixed in time. Although the interior fields, starting from artificial initial data, developed reasonably, the calculations blew up after 4 hours, probably due to the restrictive boundary conditions. When the radiation boundary conditions were used, the model ran for 6 hours, did not blow up, but developed unrealistically near the boundaries. Efforts are continuing to improve the model by introducing appropriate smoothing. Upon checkout, real data including topography, for Israel will be introduced as initial conditions.

AFOSR - 84 - 0036 - 0001

Grant Number: AFOSR 0036

THE BEHAVIOR OF THE ATMOSPHERE IN THE DESERT PLANETARY BOUNDARY LAYER

Louis Berkofsky
The Jacob Blaustein Institute for Desert Research
Ben-Gurion University of the Negev
Sede Boqer Campus 84990, Israel

14 October 1984

Final Scientific Report, 15 October 1983 - 14 October 1984
Approved for public release; distribution unlimited

Prepared for:

AIR FORCE OFFICE OF SCIENTIFIC RESEARCH
BOLLING AFB, D.C.

and

EUROPEAN OFFICE OF AEROSPACE RESEARCH AND DEVELOPMENT
LONDON, ENGLAND

TABLE OF CONTENTS

PREFACE

The research described in this report was conducted by personnel of the Jacob Blaustein Institute for Desert Research, Ben-Gurion University of the Negev, Sede Boqer, Israel from 15 October 1983 to 14 October 1984 under Grant No. AFOSR-0036 to the Ben-Gurion University of the Negev, Research and Development Authority, P.O. Box 1025, Beersheva, Israel.

Participating personnel concerned with the tasks described in this report include Prof. Louis Berkofsky, Principal Investigator, Dr. Avraham Zangvil, Research Associate, Ms. Andrea Molod, Meteorologist-Programmer, Ms. Perla Druian, Meteorologist-Programmer, and Mr. Tapani Koskela, Meteorologist-Programmer.

Observational data used in this study were obtained from the Institute's meteorological (4 m) tower, and from the radiation center, collected on a data logger and analyzed in the laboratory. Dust data were obained from the Institute's Size Selective Inlet High Volume Sampler.

The Director of the Institute during the conduct of this study was Prof. Joseph Gale.

This report should be cited as follows:

Berkofsky, L., 1984: "The Behavior of the Atmosphere in the Desert Planetary Boundary Layer," Final Scientific Report, prepared by the Desert Meteorology Unit of the Jacob Blaustein Institute for Desert Research for the U.S. Air Force Office of Scientific Research, AFSC, Bolling AFB, D.C. 20332.

INTRODUCTION

There exist a large number of planetary boundary layer models each designed for specific purposes, (Deardorff, 1974; Mahrt and Lenschow, 1976; Stull, 1976; Heidt, 1977; Yamada, 1979; Tennekes and Driedonks, 1981; Chen and Cotton, 1983). Many of these consider the top of the boundary layer a material surface. Some consider the top of the boundary layer to be coincident with the inversion, and consider entrainment across its interface. Some are multi - level, some are bulk, single - level models. The various models are of one, two and three dimensions. The greater the number of dimensions, the greater the computational complexity .

It is possible to reduce the computational complexity, and still not eliminate the three - dimensionality completely by using a variation of the "momentum integral" method (Schlichting, 1968). By means of this approach, the vertical structure of several of the variables is specified and incorporated into the vertically integrated equations. In this way, the model becomes two - dimensional in the horizontal, and vertical variations are incorporated into various coefficients. The method was introduced into meteorology by Charney and Eliassen (1979), who derived the highly successful "equivalent barotropic model". The method has also been used in studying nocturnal drainage flow (Manins and Sawford, 1979).

In this study. one of the guiding principles was that computers of limited power would be available to us. Therefore we decided at the outset to attempt to model the atmospheric circulation in the desert planetary boundary layer by means of a vertically - integrated, parameterized model.

THE MODEL AND MODEL EQUATIONS

We consider a model of the planetary boundary layer (depth approximately 1km). This layer is itself divided into a surface layer (20m), a transition layer, which at certain times and places becomes very well mixed (and is frequently called the "mixed layer") and an inversion layer. (See Figure 1). We shall not assume that the transition layer is always well mixed.

Very often, the top of the planetary boundary layer is capped by an inversion. This is particularly true in many desert and semi - desert regions. In Israel for example, there are 222 days per year, on the average, of mid-day inversions just about 100 km north of the beginning of the Negev desert. (Shaia and Jaffe 1976) As we go farther south, closer to the center of the Hadley cell, the frequency of occurrence of inversions is probably even greater. When the capping inversion exists, and when convection occurs below the inversion, the inversion changes height due to upward and corresponding downward fluxes through it by turbulence. The inversion height changes affect the dust concentration. These processes have to be modelled. Further, the processes which we wish to model are on such a scale that fairly high resolution is needed on the order of 10-20 km in the horizontal, over a region approximately 300x600 km. If then the vertical resolution above the surface layer is to be very fine - say 100m - the computation time for solution of only the boundary layer mesoscale equations may become prohibitive. Thus, in spite of the fact that the optimum mesoscale model must be three-dimensional, we expect to gain valuable insights with a vertically parameterized two-dimensional nonsteady model.

We shall concern ourselves with a form of the primitive equations derived by ensemble averaging over a horizontal area $\Delta x \Delta y$ which is large enough to contain the sub-grid scale phenomena, but small enough to be a fraction of the mesoscale system. We define

$$\left.\begin{aligned} (\overline{\alpha}) &= \frac{1}{\Delta x \Delta y}\iint \alpha \, dx\, dy \\ \alpha &= \overline{\alpha} + \alpha' \end{aligned}\right\} \qquad (1)$$

where α is any scalar variable.

With the above definitions, the appropriate equations are, approximately

$$\frac{\partial u}{\partial t} + \frac{\partial}{\partial x}(u^2) + \frac{\partial}{\partial y}(uv) + \frac{\partial}{\partial z}(uw) - f(v - v_g) = -\frac{\partial}{\partial z}\overline{(u'w')} \qquad (2)$$

$$\frac{\partial v}{\partial t} + \frac{\partial}{\partial x}(uv) + \frac{\partial}{\partial y}(v^2) + \frac{\partial}{\partial z}(vw) + f(u - u_g) = -\frac{\partial}{\partial z}\overline{(v'w')} \qquad (3)$$

$$\frac{\partial u}{\partial x} + \frac{\partial v}{\partial y} + \frac{\partial w}{\partial z} = 0 \qquad (4)$$

$$\frac{\partial \theta}{\partial t} + \frac{\partial}{\partial x}(u\theta) + \frac{\partial}{\partial y}(v\theta) + \frac{\partial}{\partial z}(w\theta) = -\frac{1}{\rho C_p}\frac{\partial F}{\partial z} - \frac{\partial}{\partial z}\overline{(w'\theta')} \qquad (5)$$

$$\frac{\partial q}{\partial t} + \frac{\partial}{\partial x}(uq) + \frac{\partial}{\partial y}(vq) + \frac{\partial}{\partial z}(wq) = -\frac{\partial}{\partial z}\overline{(w'q')} \qquad (6)$$

$$\frac{\partial c}{\partial t} + \frac{\partial}{\partial x}(uc) + \frac{\partial}{\partial y}(vc) + \frac{\partial}{\partial z}\left[(w + \Omega)c\right] = -\frac{\partial}{\partial z}\overline{(w'c')} \qquad (7)$$

In the above set of equations, the unbarred variables $u, v, w, u_g, v_g, \theta, F, P, q, c$, are all mean values according to Equation (1). We have used the Boussinesq assumption, and the variables are defined as follows:

u, v, w	=	components of the wind vector
u', v', w'	=	turbulent components of the wind vector
u_g, v_g	=	geostrophic wind components
f	=	Coriolis parameter
θ	=	potential temperature
ρ	=	air density
F	=	net radiation flux
q	=	specific humidity
c	=	dust concentration
θ', q', c'	=	turbulent fluctuations of O,q,c
x, y, z, t	=	space variables and time

c_p = specific heat of air at constant pressure

$\Omega(r)$ = fall velocity of particle of radius r

Equations (2) and (3) are the horizontal equations of motion, Equation (4) is the continuity equation, Equation (5) is the thermodynamic energy equation, Equation (6) is the moisture equation, Equation (7) is the dust concentration equation.

<u>The lower boundary condition</u> is

$$w = w_T = \mathbb{V}\cdot\nabla z_T \text{ at } z = z_T = \text{terrain height} \qquad (8)$$

Here $\mathbb{V} = \mathbf{i}\,u + \mathbf{j}\,v$ = horizontal wind vector, $\mathbf{i}$ and $\mathbf{j}$ are unit vectors in the E and N directions respectively and ∇ is the gradient operator in 2 - dimensions,

$$\nabla = \mathbf{i}\frac{\partial}{\partial x} + \mathbf{j}\frac{\partial}{\partial y}.$$

In the present investigation, we assume that any condensed moisture stays in the air. Thus we do not treat clouds or precipitation explicitly in this model (but implicit predictions are possible).

In order to expedite deriving appropriate expressions for predicting inversion height, we first derive inversion "interface" conditions. The results are essentially the <u>upper boundary conditions</u>. Let h(x,y,t) be the inversion height. Let δ be a small layer of constant thickness above the inversion level. In Mahrt and Lenschow (1976) this is called the turbulent inversion layer, which is sufficiently thin so that terms of $O(\delta)$ may be neglected in the integrated equations.

Define

$$(\tilde{\alpha}) = \frac{1}{\delta} \int_h^{h+\delta} (\alpha)\, dz \tag{9}$$

Let

$$\begin{aligned} \Delta \alpha &= \alpha_{h+\delta} - \alpha_h \\ &= \text{jump in } \alpha \text{ across inversion} \end{aligned} \tag{10}$$

By Leibniz's rule,

$$\left.\begin{aligned} &\int_h^{h+\delta} \frac{\partial \alpha}{\partial x_i}\, dz = \delta \frac{\partial}{\partial x_i} \tilde{\alpha} - \Delta \alpha \frac{\partial h}{\partial x_i} \\ &\text{where} \qquad x_i = (x,y,t) \end{aligned}\right\} \tag{11}$$

We apply the operator Equation (9) to Equations (2), (3), (5), (6), (7), allow to approach zero, and obtain.

$$\left(\frac{\partial h}{\partial t} - w_h\right)\Delta u + \Delta(u^2)\frac{\partial h}{\partial x} + \Delta(uv)\frac{\partial h}{\partial y} = -\left(\overline{u'w'}\right)_h \tag{12}$$

$$\left(\frac{\partial h}{\partial t} - w_h\right)\Delta v + \Delta(uv)\frac{\partial h}{\partial x} + \Delta(v^2)\frac{\partial h}{\partial y} = -\left(\overline{v'w'}\right)_h \tag{13}$$

$$\left(\frac{\partial h}{\partial t} - w_h\right)\Delta\theta + \Delta(u\theta)\frac{\partial h}{\partial x} + \Delta(v\theta)\frac{\partial h}{\partial y} = -\overline{(w'\theta')}_h \tag{14}$$

$$\left(\frac{\partial h}{\partial t} - w_h\right)\Delta q + \Delta(uq)\frac{\partial h}{\partial x} + \Delta(vq)\frac{\partial h}{\partial y} = -\overline{(w'q')}_h \tag{15}$$

$$\left[\frac{\partial h}{\partial t} - (w_h + \Omega)\right]\Delta C + \Delta(uC)\frac{\partial h}{\partial x} + \Delta(vC)\frac{\partial h}{\partial y} = -\overline{(w'C')}_h \tag{16}$$

In the above derivations, we have assumed that

$$\int_h^{h+\delta} \frac{1}{\rho C_p}\frac{\partial F}{\partial z}\,dz \approx \frac{1}{\delta\tilde{\rho} C_p}\left(F_{h+\delta} - F_h\right) = 0$$

and

$$(\Omega + w)_{h+\delta} = (\Omega + w)_h$$

Each of the above equations can be viewed as equations for the vertical eddy fluxes, or as prediction equations for h if these eddy fluxes are known. The quantity ($\frac{\partial h}{\partial t}$ − w_h), which represents the motion of the air relative to that of the inversion, is called the "entrainment velocity", w_e w_h is the larger scale vertical velocity at the interface. The terms involving $\partial h/\partial x$ and $\partial h/\partial y$ are usually omitted in derivations of these interface conditions, since most inversion height models assume horizontal homogeneity.

Our approach will be to integrate the system of Equations (2)-(7) inclusive, with respect to z from $z = k$ = constant = height of surface layer, to $z = h$ = inversion height, then to introduce modelling assumptions for all the variables, i., e., to specify their variations with height. If we do this, it becomes possible to express all of the jump quantities in Equations (12)-(16) inclusive in terms of their values at specific levels.

Parameterizations

Winds

Surface Layer

We assume that the surface layer is neutral, so that we may use a constant flux profile

$$V(x,y,z,t) = \frac{V_*}{k_1} \ln\left(\frac{z+z_0}{z_0}\right), \quad 0 \leq z < k \qquad (17)$$

where k_1 = von Karman constant = 0.4, V_* = friction velocity,

z_0 = roughness parameter. Here $V_* = (u_*^2 + v_*^2)^{1/2}$, where u_* and v_* are defined below.

Transition Layer:

We assume

$$u\ (x,y,z,t) = A(z)\ \hat{u}\ (x,y,t) \qquad (18)$$
$$v\ (x,y,z,t) = B(z)\ \hat{v}\ (x,y,t)$$

where

$$(\hat{q}) = \frac{1}{(h-k)} \int_k^h q\ dz \qquad (19)$$

At the level $z = k$, the two expressions (17), (18) must match

$$u(k) = \frac{u_*}{k_1} \ln\left(\frac{k+z_0}{z_0}\right) = A(k)\,\hat{u}$$

$$v(k) = \frac{v_*}{k_1} \ln\left(\frac{k+z_0}{z_0}\right) = B(k)\,\hat{v}$$

Therefore

$$\left.\begin{aligned} u_* &= \frac{k_1\, A(k)\, \hat{u}}{\ln\left(\frac{k+z_0}{z_0}\right)} \\ v_* &= \frac{k_1\, B(k)\, \hat{v}}{\ln\left(\frac{k+z_0}{z_0}\right)} \end{aligned}\right\} \qquad (20)$$

Potential Temperature

Surface Layer

Assuming that the turbulent flux of heat is also constant with height in the surface layer, we find

$$\theta\ (x,y,z,t) = \theta_{GR} + (\theta_k - \theta_{GR})\ \frac{\ln\left(\frac{z}{z_o}\right)}{\ln\left(\frac{k}{z_o}\right)} \qquad (21)$$

We derive a modelling approximation for potential temperature in regions where a nighttime inversion exists, and where surface heating during the day leads to convection and turbulent mixing. In Figure 1, an inversion exists in the early morning. The potential temperature at z = k is $\theta_{kI} = \theta(x,y,k,0)$. The potential temperature increases linearly with height according to

$$\theta(x,y,z,t) = \theta_{kI} + \gamma(0)(z-k) \qquad (22)$$

up to z=h, and linearly from there up to z = $h+\delta$, with a lapse rate $\gamma_{inv}(0)$ within the inversion layer. Here $\gamma(0)$ is also the lapse rate above the inversion layer.

Thus

$$\theta(x,y,h+\delta,t) = \theta_{h+\delta} = \theta_{kI} + \gamma(0)(z-k) + \gamma_{inv}(0)\delta \tag{23}$$

It is assumed that heating destabilizes the lapse rates, so that, at some later time

$$\left.\begin{aligned} \theta(x,y,z,t) &= \theta_k + \gamma(t)(z-k) \\ \theta(x,y,h,t) &= \theta_h = \theta_k + \gamma(t)(h-k) \end{aligned}\right\} \tag{24}$$

$$\theta(x,y,h+\delta,t) = \theta_{h+\delta} = \theta_k + \gamma(t)(h-k) + \gamma_{inv}(t)\delta \tag{25}$$

It is assumed that Equations (23) and (25) will yield the same result for $\theta_{h+\delta}$. In that case,

$$\Delta\theta = (\theta_{kI}-\theta_k) + [\gamma(0)-\gamma(t)](h-k) + \gamma_{inv}(0)\delta \tag{26}$$

From Equation (26), we see that

$$\frac{\partial}{\partial t}(\Delta\theta) = -\frac{\partial\theta_k}{\partial t} + \left[\gamma(0)-\gamma(t)\right]\frac{\partial h}{\partial t} - (h-k)\frac{\partial\gamma}{\partial t}$$

and, since

$$\frac{\partial\theta_h}{\partial t} = \frac{\partial\theta_k}{\partial t} + \gamma(t)\frac{\partial h}{\partial t} + (h-k)\frac{\partial\gamma}{\partial t}$$

from first of Equations (25), we have

$$\frac{\partial}{\partial t}(\Delta\theta) = -\frac{\partial\theta_h}{\partial t} + \gamma(0)\frac{\partial h}{\partial t} \tag{27}$$

This is similar to the result obtained by Tennekes and Driedonks (1981) for a well-mixed, horizontally homogeneous layer, i.e., "the magnitude of the temperature jump 0 increases in two ways: it increases as the height of the mixed layer increases, and decreases if the boundary layer warms up". Here we have not assumed well-mixedness ($\theta_h \neq \theta_m$) or horizontal homogeneity, so that Equation (27) is more general than was realized.

In the case of flow over water, the lapse rate $\Upsilon(t)$ is replaced by the appropriate expression for a marine environment, say $\Upsilon_1(t)$.

Moisture

We follow the same formulation as for potential temperature,

$$q(x,y,z,t) = q_k(x,y,t) + \zeta(t)(z-k) \qquad (28)$$

$$q(x,y,z,0) = q_{kI} + \zeta(0)(z-k) \qquad (29)$$

$$\Delta q = (q_{kI} - q_k) + [\zeta(0) - \zeta(t)](h-k) + \zeta_{inv}(0)\delta \qquad (30)$$

In the case of flow over water, the lapse rate of moisture $\zeta(t)$ is replaced by its appropriate value over water, say $\zeta_1(t)$.

Dust

We assume that the dust concentration is given by

$$C(x,y,z,t) = D(z)\ C_k(x,y,t) \tag{31}$$

So that

$$\Delta C = [D(h+\delta) - D(h)]\ C_k(x,y,t) \tag{32}$$

If we make the further assumption that there is no dust at the top of the inversion layer, i.e., at $z = h + \delta$, then $D(h+\delta) = 0$, (See Carlson and Prospero, 1972, concerning top of Saharan dust layer), and

$$\Delta C = -D(h)\ C_k\ (x,y,t) \tag{33}$$

Surface Parameterizations

For the momentum, we use

$$\left.\begin{aligned}\overline{(u'w')}_k &= -C_d\,[A(k)]\;|V|\;\hat{u} \\ \overline{(v'w')}_k &= -C_d\,[\,B(k)]\;|V|\;\hat{v}\end{aligned}\right\} \quad (34)$$

where C_d is the turbulent transfer coefficient for momentum, $c_d = 5\times10^{-4}\ V^{1/2}$ (V in ms^{-1}) (Berkofsky, 1982)

For the convective heating,

$$\overline{(w'\theta')}_K = C_{HO}\ A(K)\ \hat{u}\ (\theta_{GR} - \theta_k) \quad (35)$$

where θ_{GR} is the potential temperature at the ground, C_{HO} is the

For the moisture,

$$\overline{(w'q')}_k = C_{HO}\ A(k)\ \hat{u}\ [\ q_{sat}\ (\theta_{GR}) - q_k]\ \frac{W_{GR}}{W_k} \quad (36)$$

where $q_{sat}(\theta_{gr})$ means saturation mixing ratio at temperature

θ_{GR}, W_{GR} = ground soil moisture, W_k = potential saturation

value of W.

For the dust,

$$\overline{(w'c')}_k = C_d \, A(k) \, \hat{u} \, (C_{GR} - C_k) \qquad (37)$$

where C_{GR} is the dust concentration in a thin layer near the ground.

Ground Albedo

$$\alpha_{gr} = a + b \frac{W_{GR}}{W_k} \quad , b<0 \qquad (38)$$

a,b constants

In the above, W_{GR}, θ_{GR}, C_{GR} must be predicted.

Radiation

The formulation of short and longwave energy exchange in the air and at the ground is based on Gates et al (1971). The system is applied at three levels:

ground, top of surface layer, and top of transition layer: Thus the temperatures at these levels (z = 0, z = k, z = h) are needed, as is the temperature at 2m. All of these are obtainable within the framework of the model by converting potential temperatures as given to temperatures using $T = \theta\left(\frac{p}{p_o}\right)^k$

<u>Longwave</u> radiation balance (positive if upwards) at each of the three levels is defined by R_h, R_k and R_{GR} as follows:

$$\left.\begin{aligned}
R_h &= 0.736\left[\sigma T_k^4 \tau(u_\infty^* - u_k^*) + \sigma(T_a^4 - T_k^4)\frac{1+\tau(u_k^*)}{2}\right] + 0.8C_4\tau(u_k^*) \\
R_k &= 0.736\left[\sigma T_k^4 \tau(u_\infty^* - u_k^*) + \sigma(T_a^4 - T_k^4)\frac{1+\tau(u_k^*)}{2}\right] + 0.8C_4\tau(u_k^*) \\
R_{GR} &= \sigma T_a^4\left[0.6\sqrt{\tau(u_\infty^*)} - 0.1\right] + C_4
\end{aligned}\right\} \quad (39)$$

where

$$\left.\begin{aligned}
\tau(u_i^*) &= \frac{1}{1 + 1.75\,(u_i^*)^{0.416}} \\
C_4 &= \sigma\left(T_{GR}^4 - T_a^4\right) \\
T_a &= \text{temperature at 2m.} \\
\sigma &= \text{Stefan-Boltzmann constant}
\end{aligned}\right\} \quad (40)$$

u_i^* is the effective water vapor content between ground level and i, and is obtained from

$$u_i^* = \int_0^{z_i} \rho \left(\frac{p}{p_{GR}}\right) q \, dz = \frac{1}{g} \int_{p_i}^{p_{GR}} \left(\frac{p}{p_{GR}}\right) q \, dp \tag{41}$$

where p_{gr} pressure at the ground p_i = pressure at level i.

$$q = q_{GR} \left(\frac{p_i}{p_{GR}}\right)^{\lambda} , \tag{42}$$

where q_{gr} is the mixing ratio at the ground and λ = constant = 2.92 (Smith, 1966).

For levels k, h, ∞, we obtain

$$\left.\begin{aligned} u_k^* &= \frac{q_{GR}}{g\, p_{GR}^{\lambda+1}} \; \frac{p_{GR}^{\lambda+2} - p_k^{\lambda+2}}{\lambda+2} \\ u_h^* &= \frac{q_{GR}}{g\, p_{GR}^{\lambda+1}} \; \frac{p_{GR}^{\lambda+2} - p_h^{\lambda+2}}{\lambda+2} \\ u_\infty^* &= \frac{q_{GR}}{g\, p_{GR}^{\lambda+1}} \; \frac{p_{GR}^{\lambda+2} - p_\infty^{\lambda+2}}{\lambda+2} , \quad p_\infty = 120 \text{ mb} \end{aligned}\right\} \tag{43}$$

Note: if we assume $u_k^* = 0$, $\tau(u_k^*) = 1$, $\tau(u^* - u_k^*) = \tau(u_\infty)$.

Also, if we assume $T_k^4 \gg (T_a^4 - T_k^4)$, we obtain a simple form for R_k. We have not made use of these.

The effect of CO_2 absorption is taken into account by the coefficients 0.736 and the term $0.6\sqrt{\tau(u_\infty^*)} - 0.1$. The former value actually applies at 600 mb in the Mintz - Arakawa model, but we use this for h and k, which are very much lower than 600 mb. The effect of the error is not known.

Shortwave radiation (positive if downwards) is given by

$$
\left.
\begin{aligned}
S_R &= S_R^a = S_0^a \left\{ 1 - 0.271 \left[(u_\infty^* - u_R^*) \sec Z \right]^{0.303} \right\} \\
S_R &= S_R^a = S_0^a \left\{ 1 - 0.271 \left[(u_\infty^* - u_R^*) \sec Z \right]^{0.303} \right\} \\
S_{GR} &= S_{GR}^a + S_{GR}^s \\
S_{GR}^a &= (1 - \alpha_{GR}) S_0^a \left[1 - 0.271 \left(u_\infty^* \sec Z \right)^{0.303} \right] \\
S_{GR}^s &= \frac{S_0^s (1 - \alpha_{GR})(1 - \alpha_0)}{(1 - \alpha_0 \alpha_{GR})}
\end{aligned}
\right\} \qquad (44)
$$

where $S_0{}^a$ = part of the solar radiation subject to absorption = $S_0 \times 0.651 \cos Z$

$S_0{}^s$ = part of the solar radiation subject to scattering = $S_0 \times 0.349 \cos Z$

α_{gr} = ground albedo,

$\alpha_0 = \min\left\{1,\ 0.085 - 0.247 \log 10 \left[\frac{p_{GR}}{p_\infty} \cos Z \right] \right\}$ = sky albedo, (45)

Z = zenith angle of the sun

S_0 = solar constant

The radiation balance = outgoing − incoming, i.e. negative radiation balance at the ground means input of radiative heat to the surface.

Closures

At this point, we define several closure formulas, and will indicate later where and why they are used.

$$
\left.
\begin{aligned}
(\overline{w'\theta'})_h &= -A_1 (\overline{w'\theta'})_k \\
(\overline{w'c'})_h &= A^*(h) \left(\frac{\partial c}{\partial z} \right)_h \\
A^*(z) &= \begin{cases} V_* k z, & z \le k \\ \text{constant}, & k < z \le h \end{cases}
\end{aligned}
\right\}
\qquad (46)
$$

We are now in a position to derive the final form of the equations. The procedure is to apply the averaging Equation (19) to Equations (2)-(7) inclusive and use the interface conditions Equations (12)-(16) inclusive to eliminate the fluxes at inversion height, thus obtaining the transition layer equations. If we do this in all of the equations, we are left without a prediction equation for $\frac{\partial h}{\partial t}$. However if we use the first of Equations (44), which states that the turbulent flux of heat at the interface is a fraction of, and opposite in sign, to that at the top of the surface layer, in the first law of thermodynamics, this latter equation is then closed. We may then use this same (well-known, see Carson, 1973) closure in the interface Equation (14), together with the various modelling assumptions, to derive a prediction equation for $\frac{\partial h}{\partial t}$.

The ground temperature and soil moisture equations are adapted from Deardorff (1978).

The final form of the equations, in which we have used Leibniz's rule in the form

$$\int_{h}^{\ell} \frac{\partial q}{\partial x_i}\, dz = (\ell - h)\frac{\partial \hat{q}}{\partial x_i} + (\hat{q} - q_\ell)\frac{\partial \ell}{\partial x_i}\,, \quad x_i = (x, y, t) \tag{47}$$

is

<u>First Equation of Motion</u>

$$\frac{\partial \hat{u}}{\partial t} + \widehat{A^2}\,\frac{\partial \hat{u}^2}{\partial x} + \widehat{AB}\,\frac{\partial}{\partial y}(\hat{u}\,\hat{v}) - f(\hat{v} - \hat{v}_g) + \frac{\left[A(\ell+\delta)w_\ell - A(h)w_h\right]}{(\ell - h)}\hat{u}$$

$$+ \frac{\hat{u}}{(\ell - h)}\left\{ \begin{aligned} &\left[A(h) - A(\ell+\delta)\right]\frac{\partial \ell}{\partial t} + \left[A^2(h) + A^2(\ell) - \widehat{A^2} - A^2(\ell+\delta)\right]\hat{u}\,\frac{\partial \ell}{\partial x} \\ &+ \left[A(h)B(h) + A(\ell)B(\ell) - \widehat{AB} - A(\ell+\delta)B(\ell+\delta)\right]\hat{v}\,\frac{\partial \ell}{\partial y} \end{aligned} \right\} \tag{48}$$

$$= -\frac{C_d\, A(h)\,|\hat{\mathbf{V}}|\,\hat{u}}{(\ell - h)}$$

<u>Second Equation of Motion</u>

$$\frac{\partial \hat{v}}{\partial t} + \widehat{AB}\,\frac{\partial}{\partial x}(\hat{u}\,\hat{v}) + \widehat{B^2}\,\frac{\partial}{\partial y}(\hat{v}^2) + f(\hat{u} - \hat{u}_g) + \frac{\left[B(\ell+\delta)w_\ell - B(h)w_h\right]}{(\ell - h)}\hat{v}$$

$$+ \frac{\hat{v}}{(\ell - h)}\left\{ \begin{aligned} &\left[B(h) - B(\ell+\delta)\right]\frac{\partial \ell}{\partial t} + \left[A(h)B(h) + A(\ell)B(\ell) - \widehat{AB} - A(\ell+\delta)B(\ell+\delta)\right]\hat{u}\,\frac{\partial \ell}{\partial x} \\ &+ \left[B^2(h) + B^2(\ell) - \widehat{B^2} - B^2(\ell+\delta)\right]\hat{v}\,\frac{\partial \ell}{\partial y} \end{aligned} \right\} \tag{49}$$

$$= -\frac{C_d\, B(h)\,|\hat{\mathbf{V}}|\,\hat{v}}{(\ell - h)}$$

<u>First Law of Thermodynamics</u>

$$\frac{\partial \theta_\ell}{\partial t} + \frac{\partial}{\partial x}(\hat{u}\,\theta_\ell) + \frac{\partial}{\partial y}(\hat{v}\,\theta_\ell) + \frac{(\ell - h)}{2}\frac{\partial r}{\partial t}$$

$$+ \frac{\hat{u}}{(\ell - h)}\left\{\left[1 - A(\ell)\right]\theta_\ell + r\left[\widehat{A(z-h)} - A(\ell)(\ell - h)\right]\right\}\frac{\partial \ell}{\partial x} + r\left\{ \begin{aligned} &\frac{\partial}{\partial x}\left[\hat{u}\,\widehat{A(z-h)}\right] \\ &+ \frac{\partial}{\partial y}\left[\hat{v}\,\widehat{B(z-h)}\right] \end{aligned} \right\} \tag{50}$$

$$+ \frac{\hat{v}}{(\ell - h)}\left\{\left[1 - B(\ell)\right]\theta_\ell + r\left[\widehat{B(z-h)} - B(\ell)(\ell - h)\right]\right\}\frac{\partial \ell}{\partial y}$$

$$+ \frac{\theta_\ell(w_\ell - w_h)}{(\ell - h)} + w_\ell\, r = \frac{F_\ell - F_h}{\hat{\rho} C_p (\ell - h)} + \frac{(1 + A_1)\, C_{Ho}\, V_\ell\,(\theta_{GR} - \theta_\ell)}{(\ell - h)}$$

Inversion Height Equation

$$\frac{\partial h}{\partial t} = w_h - \left\{(\theta_{hI} - \theta_h) + [\gamma(0) - \gamma](h - h) + \gamma_{inv}(0)\delta\right\}^{-1} \times$$

$$\left\{ \begin{aligned} &\hat{u}\frac{\partial h}{\partial x}\Big(A(h+\delta)\,\theta_{hI} - A(h)\theta_h + A(h+\delta)\gamma_{inv}(0)\delta + (h-h)\big[A(h+\delta)\gamma(0) - A(h)\gamma\big]\Big) \\ &+\hat{v}\frac{\partial h}{\partial y}\Big(B(h+\delta)\theta_{hI} - B(h)\theta_h + B(h+\delta)\gamma_{inv}(0)\delta + (h-h)\big[B(h+\delta)\gamma(0) - B(h)\gamma\big]\Big) \\ &- A_1 C_{HO} V_h(\theta_{GR} - \theta_h) \end{aligned} \right\} \tag{51}$$

Dust Concentration Equation

$$\frac{\partial C_h}{\partial t} + \frac{\widehat{AD}}{\hat{D}}\frac{\partial}{\partial x}(C_h\hat{u}) + \frac{\widehat{BD}}{\hat{D}}\frac{\partial}{\partial y}(C_h\hat{v})$$

$$+ \frac{C_h}{\hat{D}(h-h)}\left[\hat{D}\frac{\partial h}{\partial t} + \widehat{AD}\,\hat{u}\frac{\partial h}{\partial x} + \widehat{BD}\,\hat{v}\frac{\partial h}{\partial y} - (w_h + \Omega)\right] = \frac{C_d V_*(C_{GR} - C_h)}{\hat{D}(h-h)} \tag{52}$$

Moisture Equation

$$\frac{\partial q_h}{\partial t} + \frac{\partial}{\partial x}(q_h\hat{u}) + \frac{\partial}{\partial y}(q_h\hat{v}) + \frac{\left[q_{hI} + \zeta(0)(h-h) + \zeta_{inv}(0)\delta\right]}{(h-h)} w_h - \frac{q_h w_h}{h-h}$$

$$+\left\{\frac{(h-h)[\zeta - \zeta(0)] + \zeta_{inv}(0)\delta - (q_{hI} - q_h)}{(h-h)}\right\}\frac{\partial h}{\partial t} + \frac{\zeta}{(h-h)}\left[\widehat{A(z-h)} - A(h+\delta)(h-h+\delta)\right]\hat{u}\frac{\partial h}{\partial x}$$

$$+\frac{\zeta}{(h-h)}\left[\widehat{B(z-h)} - B(h+\delta)(h-h+\delta)\right]\hat{v}\frac{\partial h}{\partial y} + \frac{(h-h)}{2}\frac{\partial \zeta}{\partial t} \tag{53}$$

$$+\zeta\left\{\frac{\partial}{\partial x}\left[\widehat{A(z-h)}\,\hat{u}\right] + \frac{\partial}{\partial y}\left[\widehat{B(z-h)}\,\hat{v}\right]\right\} = C_{HO}\,\frac{V_h\left[q_{SAt}(\theta_{GR}) - q_h\right]\frac{W_{GR}}{W_R}}{(h-h)}$$

Ground Temperature Equation

$$\frac{\partial \theta_{GR}}{\partial t} = -\frac{2\pi^{\frac{1}{2}}}{\rho_s C_s d_1} H_A - \frac{2\pi}{\tau_1}(\theta_{GR} - \theta_2) \tag{54}$$

$$H_A = \rho_h C_p C_{HO} A(h)\hat{u}(\theta_{GR} - \theta_h) - R_{NETGR}$$

Here R_{NETGR} = net radiation balance at the ground

Soil Moisture Equation

$$\frac{\partial W_{GR}}{\partial t} = -\frac{c_1 (E_g - P)}{\rho_w} - \frac{c_2 (W_{GR} - W_2)}{\rho_w \tau_1} \quad (55)$$

c_1 and c_2 are constants

ρ_w = density of liquid water

W_2 bulk moisture (analogous to θ_2)

P = precipitation rate (prescribed

ρ_s = soil density

c_s = soil specific heat

$d_1 = (k_s \tau_1)^{1/2}$

k_s = soil thermal diffusivity

τ_1 = period of 1 day

θ_2 = deep soil potential temperature

In Equations (50) and (53) above, there appear the lapse rates of potential temperature and mixing ratio, $\Gamma(t)$, and $\zeta(t)$, and their derivatives $\frac{\partial \Gamma}{\partial t}$ and $\frac{\partial \zeta}{\partial t}$. In this type of model, it is not possible to derive an equation for prediction of these quantities. Thus we have specified $\Gamma(t)$ and $\zeta(t)$. See Fig. 2 for the form of $\Gamma(t)$.

In addition to the prediction scheme, Equations (48)-(55) inclusive, there exist three diagnostic equations, two for the geostrophic wind components, and the equation of continuity for the vertical velocity.

Geostrophic Wind Equations

$$\left.\begin{aligned} \hat{u}_g &\approx -\frac{R}{f}\frac{\partial}{\partial y}\left[\theta_k + \Gamma(h-k)\right] \\ \hat{v}_g &\approx \frac{R}{f}\frac{\partial}{\partial x}\left[\theta_k + \Gamma(h-k)\right] \end{aligned}\right\} \tag{56}$$

Continuity Equation

$$w_h = w_k - (h-k)\left(\frac{\partial \hat{u}}{\partial x} + \frac{\partial \hat{v}}{\partial y}\right) - \left\{\left[1-A(h)\right]\hat{u}\frac{\partial h}{\partial x} + \left[1-B(h)\right]\hat{v}\frac{\partial h}{\partial y}\right\} \tag{57}$$

The expression for w_k is derived in the following way:
Substituting Eq. (20) into Eq. (17), we have

$$\left.\begin{aligned} u &= \frac{A(h)}{\ln\left(\frac{h+z_0}{z_0}\right)}\ln\left(\frac{z+z_0}{z_0}\right)\hat{u} \\ v &= \frac{B(h)}{\ln\left(\frac{h+z_0}{z_0}\right)}\ln\left(\frac{z+z_0}{z_0}\right)\hat{v} \end{aligned}\right\} \tag{58}$$

Then, integrating the continuity equation

$$\begin{aligned} w_h &= w_T - \int_{z_T}^{h}\left(\frac{\partial u}{\partial x} + \frac{\partial v}{\partial y}\right)dz \\ &= w_T - \left[A(h)\frac{\partial \hat{u}}{\partial x} + B(h)\frac{\partial \hat{v}}{\partial y}\right]\left[\ln\left(\frac{h+z_0}{z_0}\right)\right]^{-1}\int_{z_T}^{h}\ln\left(\frac{z+z_0}{z_0}\right)dz \end{aligned} \tag{59}$$

i.e.,

$$
\left.
\begin{aligned}
w_k &= w_T - I\left[\ln\left(\frac{k+z_0}{z_0}\right)\right]^{-1}\left[A(k)\frac{\partial \hat{u}}{\partial x} + B(k)\frac{\partial \hat{v}}{\partial y}\right] \\
I &= (k+z_0)\ln\left(\frac{k+z_0}{z_0}\right) - k
\end{aligned}
\right\} \tag{60}
$$

w_T is given by Eq. 8, and in that equation is evaluated from

$$
V_{z_T} = \frac{V_*}{k_1}\ln\left(\frac{z_T+z_0}{z_0}\right) \tag{61}
$$

Given initial values of $\hat{u}, \hat{v}, \theta_k, h, c_k, q_k, \theta_{GR}, W_{GR}$, the system can be solved. If we are concerned with a limited area, lateral boundary conditions are important. These will be discussed later. The upper and lower boundary conditions have already been prescribed.

If we assume no change of magnitude or direction of horizontal wind with height within the transition layer only, then A(z) = B(z) = 1. This situation frequently exists when the transition layer is well mixed. The equations then become:

First Equation of Motion

$$
\begin{aligned}
&\frac{\partial \hat{u}}{\partial t} + \frac{\partial}{\partial x}(\hat{u}^2) + \frac{\partial}{\partial y}(\hat{u}\hat{v}) - f(\hat{v} - \hat{v}_g) + \frac{\left[A(h+\delta)w_h - w_k\right]\hat{u}}{(h-k)} \\
&+ \frac{\hat{u}}{(h-k)}\left\{\left[1 - A(h+\delta)\right]\frac{\partial h}{\partial t} + \left[1 - A^2(h+\delta)\right]\hat{u}\frac{\partial h}{\partial x} + \left[1 - A(h+\delta)B(h+\delta)\right]\hat{v}\frac{\partial h}{\partial y}\right\} \\
&= -\frac{c_d|\hat{V}|\hat{v}}{(h-k)}
\end{aligned} \tag{62}
$$

Second Equation of Motion

$$\frac{\partial \hat{v}}{\partial t} + \frac{\partial}{\partial x}(\hat{u}\hat{v}) + \frac{\partial}{\partial y}(\hat{v}^2) + f(\hat{u}-\hat{u}_g) + \frac{[B(h+\delta)w_h - w_k]\hat{v}}{(h-k)}$$
$$+\frac{\hat{v}}{(h-k)}\left\{[1-B(h+\delta)]\frac{\partial h}{\partial t} + [1-A(h+\delta)B(h+\delta)]\hat{u}\frac{\partial h}{\partial x} + [1-B^2(h+\delta)]\hat{v}\frac{\partial h}{\partial y}\right\} = -\frac{C_d|\hat{V}|\hat{v}}{(h-k)} \tag{63}$$

First Law of Thermodynamics

$$\frac{\partial \theta_k}{\partial t} + \frac{\partial}{\partial x}(\hat{u}\,\theta_k) + \frac{\partial}{\partial y}(\hat{v}\,\theta_k) + \frac{(h-k)}{2}\frac{\partial r}{\partial t} + \frac{\theta_k(w_h - w_k)}{(h-k)}$$
$$+\frac{r}{2}(w_h + w_k) = \frac{(F_h - F_k)}{\hat{\rho}\, c_p (h-k)} + \frac{(1+A_1)\, C_{H0}\,|\hat{V}|\,(\theta_{GR}-\theta_k)}{(h-k)} \tag{64}$$

Inversion Height Equation

$$\frac{\partial h}{\partial t} = w_h - \left[(\theta_{hI}-\theta_k) + (r_I - r)(h-k) + r_{inv}(0)\delta\right]^{-1} \times$$
$$\left\{ \hat{u}\frac{\partial h}{\partial x}\Big(A(h+\delta)\theta_{hI} - \theta_k + A(h+\delta)r_{inv}(0)\delta + (h-k)[A(h+\delta)r_I - r]\Big) + \hat{v}\frac{\partial h}{\partial y}\Big(B(h+\delta)\theta_{hI} - \theta_k + B(h+\delta)r_{inv}(0)\delta + (h-k)[B(h+\delta)r_I - r]\Big) - A_1 C_{H0}|\hat{V}|(\theta_{GR}-\theta_k) \right\} \tag{65}$$

Dust Concentration Equation

$$\frac{\partial C_k}{\partial t} + \frac{\partial}{\partial x}(C_k\hat{u}) + \frac{\partial}{\partial y}(C_k\hat{v}) + \frac{C_k}{(h-k)}\left[\frac{\partial h}{\partial t} + \hat{u}\frac{\partial h}{\partial x} + \hat{v}\frac{\partial h}{\partial y} - \frac{(w_k+\Omega)}{\hat{D}}\right]$$
$$= \frac{C_d\,|\hat{V}|\,(C_{GR}-C_k)}{\hat{D}\,(h-k)} \tag{66}$$

Moisture Equation

$$\frac{\partial q_k}{\partial t} + \frac{\partial}{\partial x}(q_k \hat{u}) + \frac{\partial}{\partial y}(q_k \hat{v}) + \left[\frac{q_{kI} + \zeta(0)(h-k) + \zeta_{inv}(0)\delta}{(h-k)}\right] - \frac{q_k w_k}{(h-k)}$$
$$+ \left\{\frac{(h-k)\left[\zeta - \zeta(0)\right] + \zeta_{inv}(0)\delta - (q_{kI} - q_k)}{(h-k)}\right\}\frac{\partial h}{\partial t} + \frac{\zeta}{(h-k)}\left[\frac{(h-k)}{2} - A(k+\delta)(h-k+\delta)\right]\hat{u}\,\frac{\partial h}{\partial x} \qquad (67)$$
$$+ \frac{\zeta}{(h-k)}\left[\frac{(h-k)}{2} - B(k+\delta)(h-k+\delta)\right]\hat{v}\,\frac{\partial h}{\partial y} + \zeta\left\{\frac{\partial}{\partial x}\left[\frac{(h-k)}{2}\hat{u}\right] + \frac{\partial}{\partial y}\left[\frac{(h-k)}{2}\hat{v}\right]\right.$$
$$= C_{Ho}\,|\hat{V}|\left[q_{sat}(\theta_{GR}) - q_k\right]\frac{W_{GR}}{W_{R}}(h-k)^{-1}$$

The Ground Temperature Equation (54), Soil Moisture Equation (55), and Geostrophic Wind Equations (56) are unchanged.

The expressions for u and v in the surface layer become

$$\left.\begin{aligned} u &= \frac{\ln\left(\frac{z+z_0}{z_0}\right)}{\ln\left(\frac{k+z_0}{z_0}\right)}\,\hat{u} \\ v &= \frac{\ln\left(\frac{z+z_0}{z_0}\right)}{\ln\left(\frac{k+z_0}{z_0}\right)}\,\hat{v} \end{aligned}\right\} \qquad (68)$$

Equations of Continuity

$$\left.\begin{aligned} w_h &= w_k - (h-k)\left(\frac{\partial \hat{u}}{\partial x} + \frac{\partial \hat{v}}{\partial y}\right) \\ w_k &= w_T - I\left[\ln\left(\frac{k+z_0}{z_0}\right)\right]^{-1}\left(\frac{\partial \hat{u}}{\partial x} + \frac{\partial \hat{v}}{\partial y}\right) \end{aligned}\right\} \qquad (69)$$

From Eq. (69), we deduce

$$\left.\begin{aligned} w_k &= w_T + \frac{J\,w_h}{(h-k+J)} \\ J &= \left[\ln\left(\frac{z+z_0}{z_0}\right)\right]^{-1} I \end{aligned}\right\} \qquad (70)$$

This expression is useful in a model in which w_h is prescribed, as in the one - dimensional model to be described below. For a range of values of h ($300m \leq h \leq 2000m$), $k = 20m$, $Z_0 = 0.7cm$, and with $w_T = 0$, we find

$$-.06\, w_h \leq w_k \leq -.01 w_h$$

Thus, in this model w_k is very small, and is essentially zero, unless $w_T = 0$.

Finally, we write the equations for a model in which horizontal gradients are absent.

First Equation of Motion

$$\frac{\partial \hat{u}}{\partial t} - f\left(\hat{v} - \hat{v}_g\right) + \left[1 - A(h+\delta)\right]\frac{\hat{u}}{(h-k)}\left(\frac{\partial h}{\partial t} - w_h\right) = -\frac{C_d |\hat{V}| \hat{u}}{(h-k)} \qquad (71)$$

Second Equation of Motion

$$\frac{\partial \hat{v}}{\partial t} + f\left(\hat{u} - \hat{u}_g\right) + \left[1 - B(h+\delta)\right]\frac{\hat{v}}{(h-k)}\left(\frac{\partial h}{\partial t} - w_h\right) = -\frac{C_d |\hat{V}| \hat{v}}{(h-k)} \qquad (72)$$

First Law of Thermodynamics

$$\frac{\partial \theta_k}{\partial t} + \frac{(h-k)}{2}\frac{\partial \gamma}{\partial t} + \frac{\gamma}{2}\left(w_h + w_k\right) = \frac{\left(F_h - F_k\right)}{\hat{\rho} c_p (h-k)} + \frac{(1+A_1) C_{Ho} |\hat{V}| \left(\theta_{GR} - \theta_k\right)}{(h-k)} \tag{73}$$

Inversion Height Equation

$$\frac{\partial h}{\partial t} = w_h - \frac{A_1 C_{Ho} |\hat{V}| \left(\theta_{GR} - \theta_k\right)}{\left\{\left(\theta_{kI} - \theta_k\right) + \left[\gamma(0) - \gamma\right](h-k) + \gamma_{inv}(0)\delta\right\}} \tag{74}$$

Dust Concentration Equation

$$\frac{\partial C_k}{\partial t} + \frac{C_k}{(h-k)}\left[\frac{\partial h}{\partial t} - \left(\frac{w_h + \Omega}{\hat{D}}\right)\right] = \frac{C_d |\hat{V}| \left(C_{GR} - C_k\right)}{\hat{D}(h-k)} \tag{75}$$

Moisture Equation

$$\frac{\partial q_k}{\partial t} + \left[\frac{q_{kI} + \zeta(0)(h-k) + \zeta_{inv}(0)\delta}{(h-k)}\right] w_h + \left\{\frac{(h-k)\left[\zeta - \zeta(0)\right] + \zeta_{inv}(0)\delta - \left(q_{kI} - q_k\right)}{(h-k)}\right\}\frac{\partial h}{\partial t} = \frac{C_{Ho} |\hat{V}| \left[q_{sat}(\theta_{GR}) - q_k\right]}{(h-k)} \frac{W_{GR}}{W_h} \tag{76}$$

The Ground Temperature Equation (54) and Soil Moisture Equation (55) are unchanged. The geostrophic wind Equations (56) cannot be applied, so $\hat{u}_g, \hat{v}_g$ must be specified. Similarly, the Equations of Continuity (69) cannot be applied, so that, if an estimate of the effect of w_h is desired, w_h must be specified. Then, w_k can be deduced from Eq. (70).

THE FINITE - DIFFERENCE SCHEME

We have used a domain 300km x 60km, with Δx = 10km. Fig. 3 shows the Eliassen grid (Mesinger and Arakawa, 1976), which is a space - time grid staggered in both space and time, convenient for the leapfrog scheme associated with centered space differencing.

Two and four point averages of variable quantities were taken as needed to provide values at the grid point under consideration.

Thus averages are defined either as

$$|\overline{\alpha}^{x}|_{i,j} = \frac{1}{2}\left(\alpha_{i+\frac{1}{2},j} + \alpha_{i-\frac{1}{2},j}\right) \qquad (77)$$

or

$$|\overline{\alpha}|_{i,j} = \frac{1}{4}\left(\alpha_{i+1,j} + \alpha_{i-1,j} + \alpha_{i,j+1} + \alpha_{i,j-1}\right) \qquad (78)$$

Centered differences were taken over one or two grid intervals as dictated by locations of variables on the grid. For example, when predicting u_{ij}^{n+1}, a term like $(\partial h/\partial x)^n$ is approximated using a one-grid interval centered difference

$$(\delta_x h)_{i,j}^{n} = \frac{1}{\Delta x}\left(h_{i+\frac{1}{2},j}^{n} - h_{i-\frac{1}{2},j}^{n}\right) \tag{79}$$

When predicting $\theta_{i,j}^{n+1}$, a term like $(\partial h/\partial x)^n$ is approximated using a two-grid interval centered difference

$$(\delta_x h)_{i,j}^{n} = \frac{1}{2\Delta x}\left(h_{i+1,j}^{n} - h_{i-1,j}^{n}\right) \tag{80}$$

When a two or four point average was necessary for squared terms, the averaging operator was performed first, then the average was squared.

When a choice was necessary between one or two grid - interval differences for nonlinear terms, such as (uO), the one grid interval difference was used. All products, such as uO, were formed after appropriate averaging to provide values at the same point.

The leap-frog time differencing scheme is

$$\left.\begin{aligned} q_{i,j}^{n+1} &= q_{i,j}^{n-1} + 2\Delta t\, F_{i,j}^{n} \\ q_{i,j}^{1} &= q_{i,j}^{0} + \Delta t\, F_{i,j}^{0} \end{aligned}\right\} \tag{81}$$

LATERAL BOUNDARY CONDITIONS

We use the radiation condition proposed by Orlanski (1976). This makes use of the Sommerfeld radiation condition.

$$\frac{\partial \phi}{\partial t} + C \frac{\partial \phi}{\partial x} = 0 \tag{82}$$

where C is constant.

The finite - difference leap-frog representation of this equation is

$$\frac{\phi^{n}(JM) - \phi^{n-2}(JM)}{2\Delta t} = -\frac{C}{\Delta x}\left[\frac{\phi^{n}(JM)+\phi^{n-2}(JM)}{2} - \phi^{n-1}(JM-1)\right] \tag{83}$$

Here JM refers to the boundary point.

The essence of Orlanski's (1976) technique is: instead of fixing a constant value of the phase velocity, we numerically calculate a propagation velocity from the neighboring grid points, using the same Equation (83) for each variable to calculate C. Thus we find

$$C_{\phi} = -\frac{\left[\phi^{n}(JM-1) - \phi^{n-2}(JM-1)\right]}{\left[\frac{\phi^{n}(JM-1)+\phi^{n-2}(JM-1)}{2}\right] - \phi^{n-1}(JM-2)} \frac{\Delta x}{2\Delta t} \tag{84}$$

To determine the boundary grid point, C_ϕ from Equation (84) is substituted for C in Equation (83), in which the time index is increased by 1. We find

$$\phi^{n+1}(JM) = \left[\frac{1-\left(\frac{\Delta t}{\Delta x}\right)C_\phi}{1+\left(\frac{\Delta t}{\Delta x}\right)C_\phi}\right]\phi^{n-1}(JM) + \frac{2\left(\frac{\Delta t}{\Delta x}\right)C_\phi}{\left[1+\left(\frac{\Delta t}{\Delta x}\right)C_\phi\right]}\phi^{n}(JM-1) \tag{85}$$

In this formulation, we require $0<C_\phi\leq \Delta x/\Delta t$.

For the limiting outflow condition, $C_\phi = \Delta x/\Delta t$,

$$\phi^{n+1}(JM) = \phi^{n}(JM-1) \tag{86}$$

If $C_\phi = 0$,

$$\phi^{n+1}(JM) = \phi^{n-1}(JM) \tag{87}$$

No information has come from the interior solution when $C_\phi = 0$, so we must regard this as inflow information, to be prescribed from a previous time step.

Finally, we have:

Calculate C_ϕ from Equation (84).

$$\left.\begin{array}{l} \text{If } C_\phi > \Delta x/\Delta t \text{ (limiting outflow), set } C_\phi = \Delta x/\Delta t \\ \text{If } 0 < C_\phi < \Delta x/\Delta t \text{ (outflow), use } C_\phi \text{ as is} \\ \text{If } C_\phi < 0 \text{ (inflow), set } C_\phi = 0 \end{array}\right\} \quad (88)$$

Use C_ϕ from Equation (88) to calculate ϕ^{n+1} (JM) from Equation (85).

In our initial tests, we shall use only the condition corresponding to $C_\phi = 0$, i.e., Equation (87), on all boundaries, since this is an easy condition to apply for testing the model equations themselves.

In discussing the above, we have tacitly assumed that we are dealing with the <u>right</u> and <u>bottom</u> boundaries respectively. To derive the appropriate equations for the <u>left</u> and <u>top</u> boundaries*, we must

We have

$$\frac{\phi^{n}(JM) - \phi^{n-2}(JM)}{2\Delta t} = -\frac{c}{\Delta x}\left\{\phi^{n-1}(JM+1) - \left[\frac{\phi^{n}(JM) + \phi^{n-2}(JM)}{2}\right]\right\} \quad (89)$$

where, due to the method of indexing, JM+1 now refers to the first grid point in from the <u>left</u> and <u>top</u> boundaries. Applying Equation (89) to neighboring grid points,

*______________

when applied to the <u>top</u> and <u>bottom</u> boundaries, Δx is replaced by Δy in the set of equations.

$$C_\phi = -\frac{\left[\phi^n(JM+1) - \phi^{n-2}(JM+1)\right]}{\phi^{n-1}(JM+2) - \left[\frac{\phi^n(JM+1) + \phi^{n-2}(JM+1)}{2}\right]} \frac{\Delta x}{2\Delta t} \qquad (90)$$

We now substitute Equation (90) into Equation (89), using C_ϕ for C, and increase the time index by 1.

We obtain

$$\phi^{n+1}(JM) = \left[\frac{1+\left(\frac{\Delta t}{\Delta x}\right)C_\phi}{1-\left(\frac{\Delta t}{\Delta x}\right)C_\phi}\right]\phi^{n-1}(JM) - \frac{2\left(\frac{\Delta t}{\Delta x}\right)C_\phi}{\left[1-\left(\frac{\Delta t}{\Delta x}\right)C_\phi\right]}\phi^n(JM+1) \qquad (91)$$

In this formulation, we require $-\Delta x/\Delta t < C_\phi \leq 0$.
For the limiting outflow condition, $C_\phi = -\Delta x/\Delta t$,

$$\phi^{n+1}(JM) = \phi^n(JM+1) \qquad (92)$$

as before.

If $C_\phi = 0$,

$$\phi^{n+1}(JM) = \phi^{n-1}(JM) \qquad (93)$$

This is again regarded as inflow information.

Finally, we have:

Calculate C_ϕ from Equation (90).

$$
\begin{aligned}
&\text{If } C_\phi < -\Delta x/\Delta t, \text{ (limiting outflow), set } C_\phi = -\Delta x/\Delta t \\
&\text{If } -\Delta x/\Delta t < C_\phi \leq 0, \text{ (outflow), use } C_\phi \text{ as is.} \\
&\text{If } C_\phi > 0 \text{ (inflow), set } C_\phi = 0
\end{aligned}
\tag{94}
$$

Use C_ϕ from Equation (94) to calculate ϕ^{n+1} (JM) from Equation (91).

In the above Equations (84) and (90), it is conceivable that C_ϕ may become infinite or indeterminate.

<u>Case 1 - C_ϕ infinite</u>

Equation (85) may be written

$$\phi^{n+1}(JM) = \left[\frac{\frac{1}{C_\phi} - \left(\frac{\Delta t}{\Delta x}\right)}{\frac{1}{C_\phi} + \left(\frac{\Delta t}{\Delta x}\right)}\right] \phi^{n-1}(JM) + \left[\frac{2\left(\frac{\Delta t}{\Delta x}\right)}{\frac{1}{C_\phi} + \left(\frac{\Delta t}{\Delta x}\right)}\right] \phi^{n}(JM-1) \tag{95}$$

$$\lim_{C_\phi \to \pm\infty} \phi^{n+1}(JM) = 2\phi^{n}(JM-1) - \phi^{n-1}(JM) \tag{96}$$

Similarly, Equation (91) becomes

$$\lim_{C_\phi \to \pm\infty} \phi^{n+1}(JM) = 2\phi^{n}(JM+1) - \phi^{n-1}(JM) \tag{97}$$

Case 2 - C_ϕ indeterminate

This situation arises when, in addition to the fact that the denominator of Equation (84) is zero, the numerator is also. then

$$\phi^n\ (JM-1) = \phi^{n-2}\ (JM-1) \quad . \tag{98}$$

If applied to the boundary point (JM), this is essentially the statement Equation (87) corresponding to $C_\phi = 0$. Thus, in case the numerator of Equation (84) or Equation (90) is zero, we use the condition corresponding to $C_\phi = 0$, i.e., Equation (87) or Equation (93).

EXPERIMENTS

One - Dimensional

Our initial experiments are all concerned with a dry atmosphere. We first ran the one - dimensional model, given by Equations (71)-(75) inclusive plus Equation (54), with the following conditions:

$A\ (h+\zeta) = B\ (h+\zeta) = 1$ (no wind-shear across inversion)

$\hat{u}_g = \hat{v}_g = 0$ (no geostrophic wind)

a.) $w_h = 0;\ w_k = 0$

b.) $w_h = -\ (h-k)\left(\frac{\partial \hat{u}}{\partial x} + \frac{\partial \hat{v}}{\partial y}\right) = -(h-k)\ B$ (B = constant); $w_k = 0$

$B = -5\times10^{-5}s^{-1}(0900-1500)$

$-5\times10^{-5}s^{-1} + 5\times10^{-5}s^{-1}(1500-2100)$

$5\times10^{-5}s^{-1}(2100-0300)$

$5\times10^{-5}s^{-1} - 5\times10^{-5}s^{-1}(0300-0900)$

c.) $\hat{u} = \hat{v} = 100$ cm s^{-1}

d.) $\theta_k = 303\ ^{o}K$, $\theta_{GR} = 303.2^{o}k$

e.) $C_{ho} = 4 \times 10^{-2}$

f.) $h_o = 300$ m

g.) $C_k = 100\ \mu gm^{-3}$

h.) $C_{GR} = 100\ \mu gm^{-3}$ = constant;

i.) $C_{GR} = 10{,}000\ \mu gm^{-3}$ = constant

The results of the experiment with $w_h = 0$ are shown in Figures 4, 5, and 6.

Figure 4 shows the evolution of the fields of $\hat{u}$ and $\hat{v}$ (the caps are omitted from the figure). These fields evolve smoothly. The absolute value of the wind reaches a maximum at about 1300 LST and a minimum at about 0100 LST. Fig. 5 shows the evolution of the ground temperature θ_{GR} and the temperature at the top of the surface layer θ_k. θ_{GR} reaches its maximum value at about 1400, while θ_k reaches its maximum at about 1600 local time. Both of these are reasonable. The ground temperature reaches its minimum at about 0600, while the air temperature reaches its minimum at about 0800, which is somewhat late. The maximum and minimum of θ_{GR} both exceed the corresponding values for, θ_k which is realistic. The range of both values is somewhat less than should be expected on a summer day with light winds.

Figure 6 shows the evolution of the inversion height (H in the figure) and dust concentration C_k for the two cases,

$C_{GR} = 100\,\mu gm^{-3}$, $C_{GR} = 10{,}000\,\mu gm^{-3}$.

The former of these corresponds to an average air value for Saharan dust. It turned out, after 6 months of observation at Sde Boqer, that the average value is closer to $60\,\mu gm^{-3}$. However, the use of 100 will not alter these results in any substantial way. The value $10{,}000\,\mu gm^{-3}$ corresponds to that within a strong dust storm. The first thing that can be seen from this figure is that the inversion height rises steadily throughout the day. This may be indicative of the fact that a convective boundary layer model should apply only during daylight hours - or it may indicate that subsidence at inversion level is required to bring the inversion down at night.

The curve $C_{GR} = 100\,\mu gm^{-3}$ shows the trend of C_k (dust concentration at 20 meters). This quantity decreases steadily with time. This is not surprising, since, according to Equation (75), the tendency of C_k is inversely proportional to the inversion height. It also indicates that the turbulent transport of dust was too weak to overcome the thinning out of C_k as the inversion rose. With $C_{GR} = 10{,}000\,\mu gm^{-3}$, there is continuous intense turbulent transport, so that the dust concentration at z = k is kept high throughout the period.

It should be recalled that both Θ_k and h are dependent upon the assumed form of $\Gamma(t)$ (Figure 2). Thus, it is possible to "tune" the model by experimenting with other curves of $\Gamma(t)$.

Figures 7, 8, 9 shows the results for the same quantities when w_h, the vertical velocity at inversion height, is not zero. In actual fact, this quantity should be obtained by solving the continuity equation, which is not available in a model without horizontal transport. Thus we assume values of the horizontal divergence B (given in the list of data), which vary with time throughout the day. Again, this quantity is "tunable", but we wish to highlight the effect of subsidence on inversion height.

Figure 7 shows the evolution of $\hat{u}$ and $\hat{v}$ when $w_h \neq 0$. The results are indistinguishable from those of Figure 4. This is simply because the w_h terms vanish from Equations (71) and (72) under the conditions we have assumed.

Figure 8 shows the evolution of θ_{GR} and θ_k. There are some small differences between these results and those with $w_h = 0$, but the evolution is more or less the same in both cases.

The major differences in the case $w_h \neq 0$ can be seen in Figure 9, when compared with Figure 6. Figure 9 shows the evolution of inversion height, h, and of dust concentration, C_k. The inversion height now reaches a maximum of about 1400 m at about 1800 LST, and then falls due to subsidence. It reaches a minimum of about 600 m at about 0500, and then starts up again. Even though the value itself at the minimum may not be realistic, this experiment very strongly highlights the effect of the vertical velocity at inversion height level on the inversion height itself.

The same type of result is true for C_k. For $C_{GR} = 100 \mu gm^{-3}$, there is little change in C_k, except that it does not decrease as much as it did in the case $w_h = 0$. This is so because the subsidence during the latter part of the period tends to increase the concentration at lower levels.

This effect is even more marked in the case of $C_{GR} = 10{,}000 \mu gm^{-3}$. There is intense turbulent transport upward during the entire period. During the second half of the day, the upward transport to level z=k is intensified by subsidence to that level, so that C_k continues to increase.

It should be realized that the assumption of C_{GR} = constant for 24 hours is rather weak, in the sense that wind erosion, which causes variations in C_{GR}, occurs in bursts. We shall discuss this point later.

The legends at the top of all the figures contain the heading "NON -

PARAMETERIZED DUST EQ." We have distinguished these results from results with "PARAMETERIZED DUST EQ", to be shown below, for the following reasons.

We have used the interface Equations (12)-(16) inclusive, to eliminate the turbulent fluxes, at z=h except for Equation (14). It is also possible to parameterize the other fluxes, for example $\overline{(w'c')}_h$ in Equation (16). If we use the flux - gradient relation

$$-\overline{w'c'} = A^*(z) \frac{\partial c}{\partial z} \tag{99}$$

then $$-\overline{(w'c')}_h = A^*(h) \; D'(h) c_k \tag{100}$$

where $A^*(z)$, the coefficient of eddy diffusion, is given by Equation (46).

In that case, Equation (16) becomes

$$\frac{\partial h}{\partial t} = (w_h + \Omega) - \frac{A^* D'(h)}{D(h)} \tag{101}$$

and the dust concentration equation becomes

$$\frac{\partial C_k}{\partial t} + \frac{[\hat{D} - D(h)]}{\hat{D}(h-k)} C_k \frac{\partial h}{\partial t} + \frac{[D(h)-\hat{D}] w_h + (\hat{D}-1) w_k + [D(h)-1]\Omega}{\hat{D}(h-k)}$$
$$= \frac{C_d |\hat{V}| (C_{Gk} - C_k) + A^* D'(h) C_k}{\hat{D}(h-k)} \tag{102}$$

instead of Equation (75). We now see that the model in this form contains two inversion height equations, Equation (74) due to convection of heat and Equation (102) due to turbulent diffusion of dust. We carried out experiments with the same initial data , but in which the inversion height was calculated as an average of the results from Equation (74) and (102). The results are shown in Figures 10-15 inclusive. The major differences between these results and the non-parameterized results are in the inversion heght and dust calculations, seen in Figures 12 and 15. These should be compared with Figures 6 and 9 respectively. For the $w_h = 0$ case, the results show similar trends, but the non - parameterized inversion height went much higher, and the curve is less smooth. This is undoubtedly due to the averaging involved in obtaining the parameterized height. The variation of C_k is quite similar in both cases, although when $C_{GR} = 10{,}000\,\mu gm^{-3}$, C_k does not drop down, in the parameterized case as it did in the non-parameterized case. When $w_h \neq 0$ the curves look quite similar, except that the maxima and minima of inversion height occur about an hour later in the parameterized case than in the non-parameterized case.

The conclusion to be drawn from these comparisons is that the non-parameterized system, which is theoretically more correct, should be used.

Two - Dimensional Experiments

We used the system of Equations (62) - (66) inclusive, Equations (68), (69), (70). We have not assumed $A\ (h+\delta)$, $B\ (h+\delta) = 0$, i.e., we have allowed wind shear through the inversion.

a). Constant Boundary Conditions

We consider a region 300km x 600km, with a grid spacing $\Delta x = \Delta y =$ 10km. In this experiment, we used the lateral boundary condition corresponding to $C_\phi =$ 0, i.e.,

$$\phi^{n+1}(JM) = \phi^{n-1}(JM) \qquad (87)$$

Thus we expect that this fixed boundary condition will eventually lead to instability due to reflection at the boundaries.

As this experiment was essentially a check of the program, we used very simple initial conditions.

$\hat{u}$ = 100 cm s^{-1} everywhere

$\hat{v}$ = 0

h = 650 m

θ_k = 303°k

θ_{GR} = $303.^{\circ}2$k

$\gamma(t)$ as in Figure 2.

C_k = $100 \mu gm^{-3}$

C_{GR} = $100 \mu gm^{-3}$

$A(h+\delta) = B(h+\delta) = 1.01$ – corresponding to $1ms^{-1}$ $(10m)^{-1}$

$\hat{u}_g$ was taken as 1 ms^{-1}

$\hat{v}_g = 0$

We expect changes in the variables due to changes in the radiation fluxes.

We used a time step of Δt = 1 minute. When the program ran smoothly for 33 time steps, we tried Δt = 2 minutes, with identical results. We then ran for a longer period, but the calculations blew up at time step 122 = 4.07 hours, primarily due to boundary instability. The evolution of the interior fields seemed reasonable.

b.) Radiation Boundary Conditions

Starting from the same initial fields, we applied the radiation conditions Equations (82) – (98) inclusive. The experiments have been run so far for 6 hours, with one minute time steps. The evolution of the interior fields seemed reasonable. Strong gradients did not develop in all the interiors as they did in the constant boundary condition case.

c.) Comparison of Results of the Two Experiments

In the figures to be discussed below, we have displayed the printouts for the various fields, only for rows 1,2,3,4,5,58,59,60,61. The remaining fields are smooth transitions. Due to the printing limitations, each row of the grid is represented by almost two full rows on the printout, so that columns 1 through 17 go from left to right, while columns 18 through 31, just beneath them, go from right to left. We have since modified the print routine to give a clear rectangular array, and future results will be printed in the manner.

Figure 16 shows the ϕ-field at 180 minutes, with constant boundary conditions. Fig. 17 shows the $\hat{\phi}$-field with radiation boundary conditions. Although the numbers on the bottom boundary of the latter are larger than in the constant B.C. case, the fields everywhere else are quite uniform and smooth. Figures 18 and 19 show the $\hat{v}$-fields in the constant and radiation cases. Again, the interior fields in the radiation case are much smoother, and less subject to gradients created by boundary reflection. The inversion heights are shown in Figures 20 (constant) and 21 (radiation). There is no question of the superiority of the radiation condition for this field, even though the left and upper boundaries are not sufficiently smooth. Figures 22 and 23 show the θ_k fields in the constant and radiation cases. Except for the bottom row, the radiation condition gives a smoother field. Figures 24 and 25 show θ_{GR} in the constant and radiation cases. Again, the radiation case is clearly superior. Figures 26 and 27 show the C_k (dust) fields in the constant and radiation cases. In this field, the interior for the constant case alredy shows large, unrealistic values, while these values for the radiation case are very smooth. Finally, Figures 28 and 29 show the w_h values and radiation cases. These values should all be zero, as both $\hat{u}$ and $\hat{v}$ should be developing uniformly. While all are very small, the fields in the constant case are already beginning to develop, while they are almost all zero in the radiation case.

These results clearly illustrate the efficacy and superiority of the radiation boundary condition over the constant boundary condition. Yet the boundaries still require additional treatment. We plan to experiment with suitable filters (Shapiro, 1975) to control spurious high frequency oscillations on the boundaries themselves. There are also suggestions (Miller and Thorpe, 1981) for improved versions of the radiation boundary condition.

As noted earlier, the radiation boundary condition experiments have been continued for 6 hours, with one minute time steps. All of the fields developed reasonably, with little encroachment from the boundaries, except the inversion height field. While the calculations still did not blow up at 6 hours, spurious oscillations were developing in this field. It is clear that some kind of smoothing is required. This will be attempted in future experiments.

CONCLUSIONS

The one - and two - dimensional versions of the desert planetary boundary layer model appear to be checked out, in the sense that they give reasonable metereological results.

The one - dimensional version runs well for 24-hours, and can certainly be run for longer periods. It is now possible to use this model for a number of sensitivity experiments, such as prescription of dust concentration at the ground as a function of time, variable vertical velocity at inversion height, variable surface albedo.

The two - dimensional version runs well for up to 6 hours before fluctuations in the inversion height field set in. Thus, more numerical investigation is needed in order to carry the experiments further. As already stated above, the investigations will take the form of smoothing and filtering operators, and possible improved forms of the radiation boundary conditions.

We have already prepared a set of base data of all fields for Israel, and will carry out experiments with these data, over irregular terrain, following adoption of more suitable numerical techniques.

RECOMMENDATIONS

There are a number of steps which can be taken which may lead to improvement of the present model. Although the model appears to be checked out, in the sense that it does not blow up by 6 hours, and gives reasonable evolution of the fields during that time it is desirable to focus on a model which may be useful operationally.

There are still several steps which may be taken to improve the radiation boundary conditions. Among them are the application of a suitable filter (Shapiro,1975), which was successfully applied to this type of problem by Eliassen and Thorsteinsson (1984). Another is the possibility of applying an improved version of the radiation boundary condition according to the method suggested by Miller and Thorpe (1981).

There are also several ways of improving the physics in the dry model. We could try a possibly more realistic version of the stability $\gamma(t)$. We could also try to improve the assumption that the dust concentration near the ground, C_{GR}, is constant. To do so requires a method for predicting erosion of soil by wind . A first step in this direction has been taken by Berkofsky (1984) who developed an equation describing the processes of detachment, transport and deposition which make up wind erosion.

When all of the above has been incorporated we can then include moisture and a thermally active surface layer. Real data (already compiled for Israel for this model) can then be used as input, together with topography, for operational testing.

Finally, it is possible to combine this model with that of the free atmosphere for a simplified version of a tropical operational model. Such a model has been suggested by Berkofsky (1983).

DUST CONCENTRATION DATA

In Table 1 we present dust concentration data for Sede Boqer, compiled simce June 1984. For a variety of technical reasons, the data are not continuous. These dust concentration data were obtained with an ultra - high volume sampler (Sierra Instruments) with cascade impactor, with a constant flow meter operating at 40 cubic feet per minute. These categories are:

C_1 : 7.2 - ∞ μ

C_2 : 3.0 - 7.2 μ

C_3 : 1.5 - 3.0 μ

C_4 : 0.95 - 1.5 μ

C_5 : 0.49 - 0.95 μ

C_6 : < 0.49 μ

The averages in μgm^{-3}, are:

Total	C_1	C_2	C_3	C_4	C_5	C_6
59.81	11.24	15.23	12.13	10.26	5.98	18.71

The minimum value was 10.47 μgm^{-3} on 11/11/84. The maximum value was 133. 20 μgm^{-3} on 1/8/84. The wind direction is given as a sort of twenty - four hour average. It is seen that westerly winds dominate.

These data will have to be analyzed with respect to the prevailing synoptic situation.

Table 1. - Dust Concentration Data at Sede Boqer.

DATE	TOT.C ($\mu gr/m^3$)	C1 ($\mu gr/m^3$)	C2 ($\mu gr/m^3$)	C3 ($\mu gr/m^3$)	C4 ($\mu gr/m^3$)	C5 ($\mu gr/m^3$)	C6 ($\mu gr/m^3$)	V (m/sec)	V(dir)
17-06-84	54.98	11.03	12.25	2.93	2.93	5.79	20.05	4.5	N/W
20-06-84	66.08	18.85	24.24	3.19	1.25	4.70	13.84	4.4	N/W
28-06-84	63.88	15.75	18.91	5.49	7.93	10.92	11.54	4.5	N/NW/SW
01-07-84	43.25	5.69	8.21	3.10	2.64	4.94	18.67	4.0	NW/W
02-07-84	72.95	10.00	14.67	5.79	5.59	7.10	29.80	4.3	N/NNW/NW/W/E
04-07-84	79.26	17.69	6.35	2.79	5.18	14.77	35.68	4.0	N/NW/W/SE/E
08-07-84	55.33	13.20	14.20	4.53	3.74	6.74	12.93	4.2	NW/W
09-07-84	68.73	18.02	20.88	5.97	4.65	7.34	11.87	4.7	N/NW/W
10-07-84	57.54	15.83	16.25	4.30	3.64	6.33	11.17	4.6	NW
11-07-84	58.34	11.79	14.59	3.57	3.27	5.83	19.29	4.7	NW/SW
12-07-84	43.57	6.45	8.70	3.04	2.25	3.83	19.29	4.4	NW/W/SW
15-07-84	51.36	6.63	7.33	2.44	3.84	5.41	25.71	4.1	NW/SW
16-07-84	57.46	9.65	11.05	2.93	3.91	5.56	24.36	4.1	NW/W
17-07-84	57.30	7.25	10.01	4.26	4.55	4.50	26.73	4.3	N/NW/W/SW/S
18-07-84	60.68	6.70	8.85	2.45	3.09	3.14	36.45	4.5	N/NW/SW
19-07-84	73.17	9.04	14.46	7.01	5.48	7.63	29.55	5.1	NW
22-07-84	80.90	14.38	19.71	5.57	6.16	10.83	24.06	4.7	NW/W
24-07-84	83.64	15.16	24.51	7.64	7.83	10.80	17.69	4.4	NW/W
25-07-84	86.66	17.34	23.04	7.14	6.72	10.08	20.34	4.8	NW/W
26-07-84	77.15	12.78	15.14	5.87	8.18	12.35	22.83	3.9	N/NW/W
29-07-84	70.02	14.50	15.11	5.84	4.98	10.32	19.29	4.5	NW/W
30-07-84	79.59	19.03	21.67	4.64	5.70	9.04	19.50	4.8	NW/W
31-07-84	60.54	13.08	3.60	4.61	15.23	8.85	15.17	4.9	N/NW
01-08-84	133.20	31.83	35.17	9.04	7.07	9.63	10.47	6.6	N
09-08-84	51.67	6.47	13.13	4.44	4.19	7.60	16.52	4.6	N/NW/W
14-08-84	50.46	7.52	16.89	5.46	2.88	4.20	13.51	5.4	N/NW/SW
19-08-84	35.55	7.01	13.36	4.07	2.31	5.16	3.65	4.7	NW/W
21-08-84	42.61	7.15	11.93	3.71	2.97	6.00	10.85	4.2	NW/W
22-08-84	43.84	5.45	12.32	3.95	3.40	7.01	11.71	4.3	NW/W
26-08-84	36.29	3.97	5.85	2.47	2.15	2.93	18.92	3.0	N/NW/VAR
29-08-84	57.54	10.46	12.50	4.15	5.16	8.15	17.12	4.6	NW/W
30-08-84	46.31	3.86	7.11	5.94	6.42	1.24	21.74	4.5	N/W
02-09-84	61.06	12.76	18.21	4.42	3.38	5.93	16.35	4.2	NW/W
03/4-09-84	90.30	14.01	20.59	23.72	4.00	6.44	21.54	4.1	NW/SW
05/6-09-84	73.72	13.53	18.28	3.61	3.07	4.75	30.48	3.8	NW/W
09-09-84	60.31	9.59	9.85	4.03	4.83	7.41	24.60	3.9	NW
17-09-84	74.47	14.42	18.45	5.62	5.82	0.99	29.17	4.2	N/NW
19-09-84	102.96	17.96	23.65	6.89	6.31	7.46	40.69	4.5	NW/W
30-09-84	47.76	11.45	13.14	4.08	2.19	3.54	13.35	4.3	NW/W
01-10-84	57.67	15.68	20.52	5.63	2.74	4.21	8.89	4.6	N/NW
07-10-84	57.16	6.31	19.40	6.83	3.96	3.67	16.99	4.5	NW/SW
08-10-84	50.13	8.62	13.21	4.64	4.08	4.13	15.45	4.7	NW
28-10-84	42.80	9.02	12.84	3.31	2.34	3.71	11.58	3.8	N/NW/W
30-10-84	111.34	18.50	47.93	15.43	7.66	5.07	16.75	4.6	NW/W
31-10-84	42.00	6.21	18.18	6.89	2.71	2.65	5.36	4.0	NW
04-11-84	52.30	8.32	14.83	4.35	4.08	4.85	15.87	4.6	NW/SW
05-11-84	23.57	4.82	7.01	2.08	0.93	2.43	6.30	3.6	NW/W
06-11-84	49.81	9.07	13.58	2.96	2.65	6.98	14.57	3.9	NW/W/SW
11-11-84	10.47	2.26	2.42	1.00	1.16	2.00	1.63	3.2	NW/W
12-11-84	26.08	5.95	7.21	2.34	1.80	3.31	5.47	3.5	N/NW

Bibliography

1. Deardorff, J., 1974: Three-Dimensional Numerical Study of the Height and Mean Structure of a Heated Planetary Boundary Layer, Boundary Layer Meteor., 7, 81-106.

2. Mahrt, L. and D.H. Lenschow, 1976: Growth Dynamics of the Convectively Mixed Layer, J. Atmos. Sci. , 33, 41-51.

3. Stull, R.B.,1976: The Energetics of Entrainment Across a Density Interface, J. Atmos. Sci. , 33, 1260-1267.

4. Heidt, F.D., 1977: The Growth of the Mixed Layer in a Stratified Fluid Due to Penetrative Convection, Boundary Layer Meteorology , 12, 439-461.

5. Yamada, T., 1979: Prediction of the Nocturnal Surface Inversion Height, J. Appl. Meteor. 18, 526-531.

6. Tennekes, H. and A.G.M. Dreidonks, 1981: Basic Entrainment Equations for the Atmospheric Boundary Layer, Boundary Layer Meteorology , 20, 515-532.

7. Chen, C. and W.R. Cotton, 1983: Numerical Experiments With a One-Dimensional Higher Order Turbulence Model: Simulation of a Wangara Day 33 Case, Boundary Layer Meteorology , 25, 375-404.

8. Schlichting, H., 1968. Boundary layer Theory , 747 pp., McGraw-Hill, New York.

9. Charney, J.G. and A. Eliassen, 1949: A Numerical Method for Predicting the Perturbations of the Middle Latitude Westerlies, TELLUS , 1, 38-54.

10. Manins, P.C. and B.L. Sawford, 1979: A Model of Katabatic Winds. J. Atmos. Sci., 36, 619-630.

11. Shaia, J.S. and S. Jaffe, 1976: Midday Inversion Over Bet-Dagan, Israel Meteorological Service, Bet Dagan, Israel, Series S (Meteorological Notes) No. 33.

12. Carlson, T.N. and J.M. Prospero, 1972: The Large-Scale Movement of Saharan Air Outbreaks Over the Northern Equatorial Atlantic, JAM, Vol. 11, No. 2, 283-297.

13. Berkofsky, L., 1982: A Heuristic Investigation to Evaluate the Feasibility of Developing a Desert Dust Prediction Model. Mon. Wea. Rev., 110, 2055-2062.

14. Gates, W.L. E.S. Batten, A.B. Kahle and A.B. Nelson, 1971: A Documentation of the Mintz - Arakawa Two-Level Atmospheric General Circulation Model: A Report Prepared for Advanced Research Projects Agency, Rand Corporation, Santa Monica, California, U.S.A., 408 pp.(ARPA order No. 189-1), R-877-ARPA.

15. Smith, W.L. 1966: Note on the Relationship Between Total Precipitable Water and Surface Dew Point, JAM, V.5, No. 5, 726-727.

16. Carson, D.J., 1973: The Development of a Dry Inversion - Capped Convectively Unstable Boundary layer, Ouart. J.R. Met. Soc., 99, 450-467.

17. Deardorff, J.W. 1978: Efficient Prediction of Ground Surface Temperature and Moisture With Inclusion of a Layer of Vegetation, J. Geophys. Res., 1889-1902.

18. Mesinger, F. and A. Arakawa, 1976: Numerical Methods Used in Atmospheric Models, GARP PUBLICATIONS SERIES No. 17, V.1, pp. 53.

19. Orlanski, I., 1976: A Simple Boundary Condition for Unbounded Hyperbolic Flows, J. Comp. Phys., 21, 251-269.

20. Shapiro, R. 1975: Linear Filtering, Mathematics of Computation, 29, 1094-1097.

21. Eliassen, A. and S. Thorsteinsson, 1984: Numerical Studies of Stratified Air Flow Over A Mountain Ridge on the Rotating Earth. TELLUS, 36, 173-187.

22. Miller, M.J. and A.J. Thorpe, 1981: Radiation Conditions for the Lateral Boundaries of Limited Area Numerical Models, Quart J.R. Meteorology Soc., 107, 615-628.

23. Berkofsky, L., 1984: Wind Erosion, paper presented at Ben-Gurion University - U.C.L.A. Conference on Desert Research held at Sede Boqer, Israel, 16-21 Sept. 1984, 19 pp.

24. Berkofsky, L. 1983: Tropical Limited Area Modelling: A Background Study, World Meteorological Organization, Geneva, 75 pp.

ACKNOWLEDGMENTS

The program was prepared by Andrea Molod, assisted by Perla Druian. The final checkout was accomplished by Tapani Koskela, a visitor from University of Helsinki. The suggestions and discussions with all of the above contributed substantially to the development of the model in its present form . The typing was done by Dina Feingold. The assistance of all of these people is gratefully acknowledged.

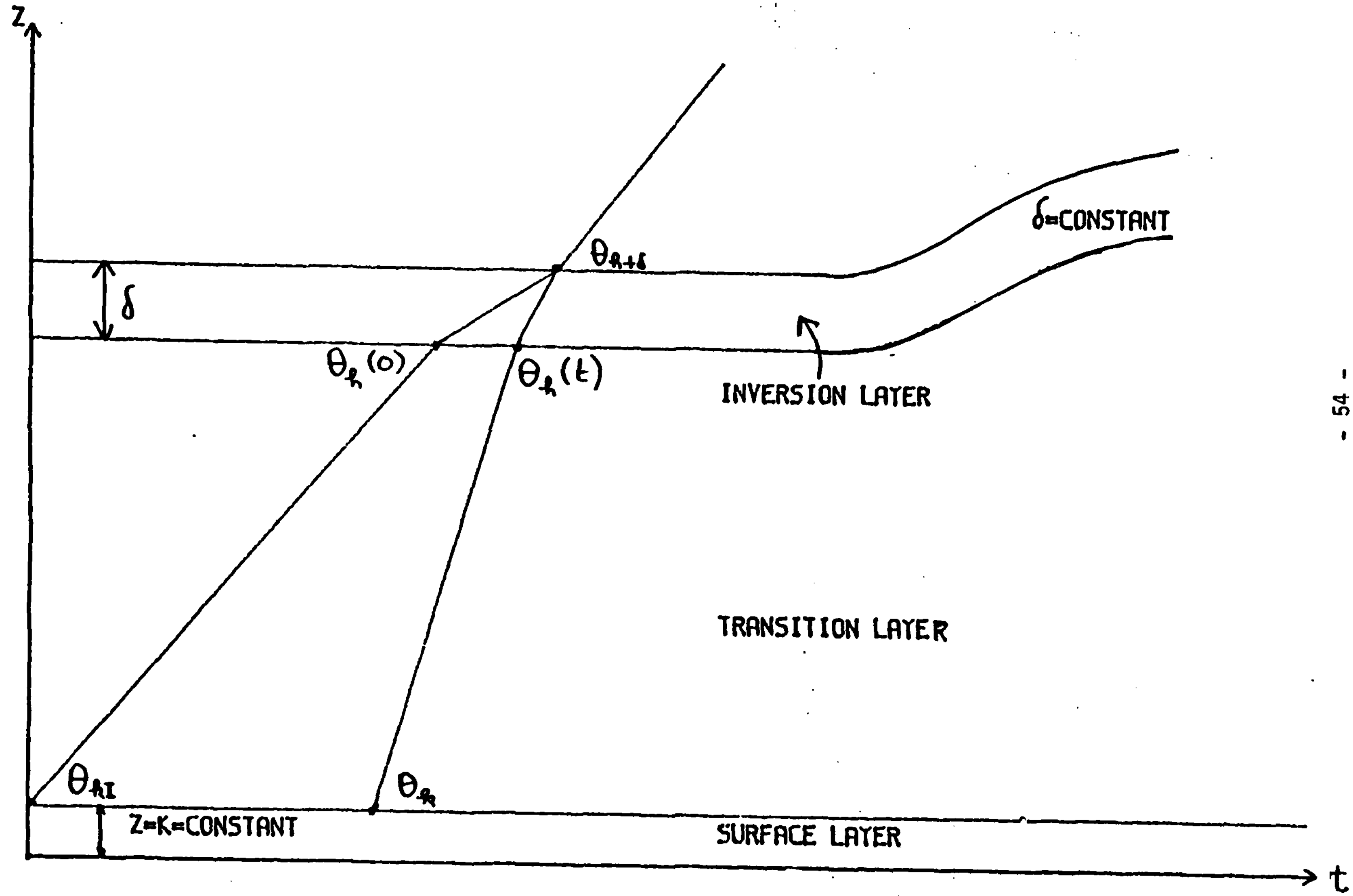

Fig. 1 – Schematic of Planetary Boundary Layer.

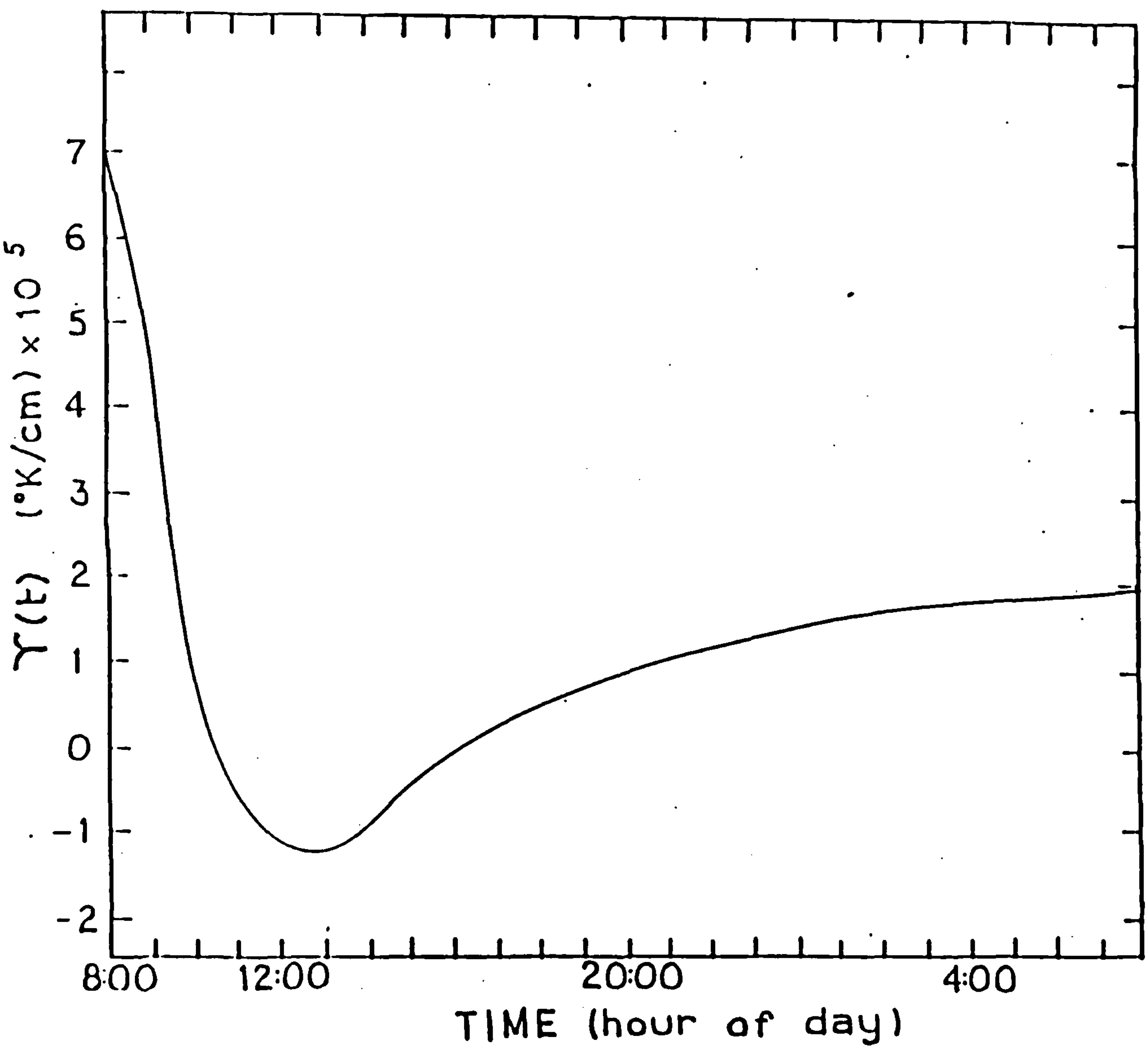

Fig. 2. - The Lapse-Rate $\Upsilon(t)$.

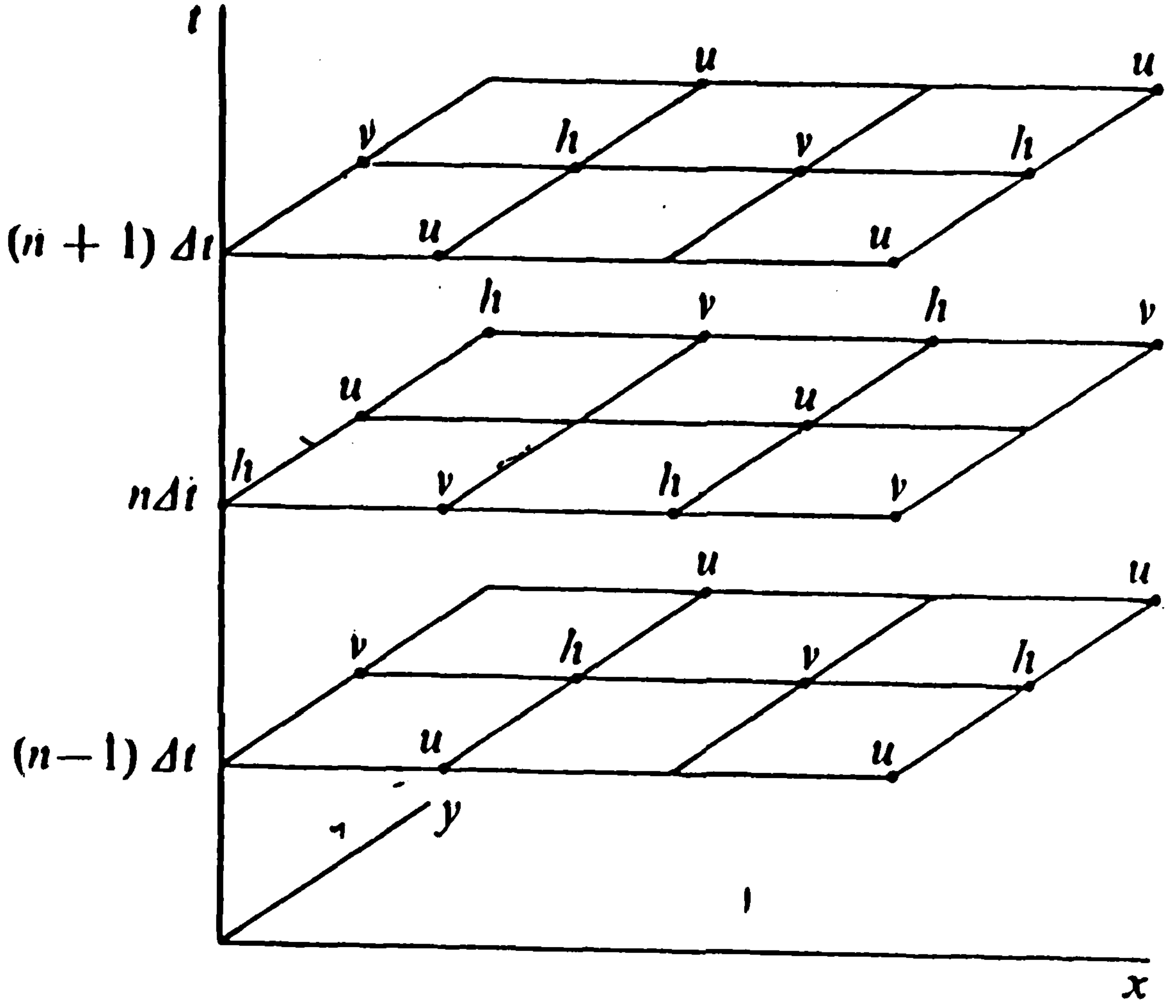

Fig. 3. - Space-time Grid Staggered Both in Space and Time, Convenient for the Leapfrog Scheme Associated with Centered Space Differencing (after Eliassen, 1956).

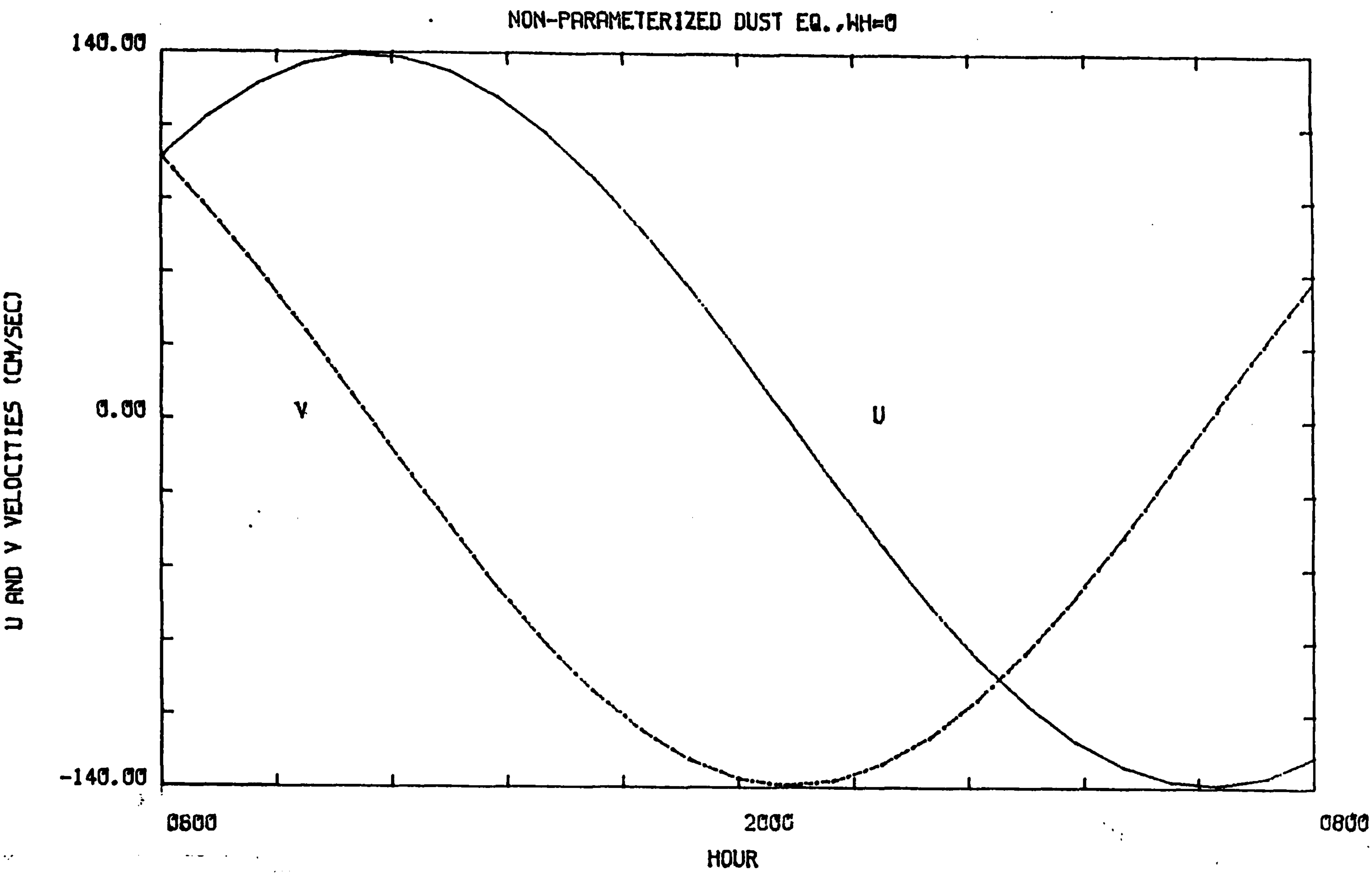

Fig. 4. – Evolution of $\hat{u}$ and $\hat{v}$ from One-Dimensional Non-Parameterized Dust Model, $w_h = 0$.

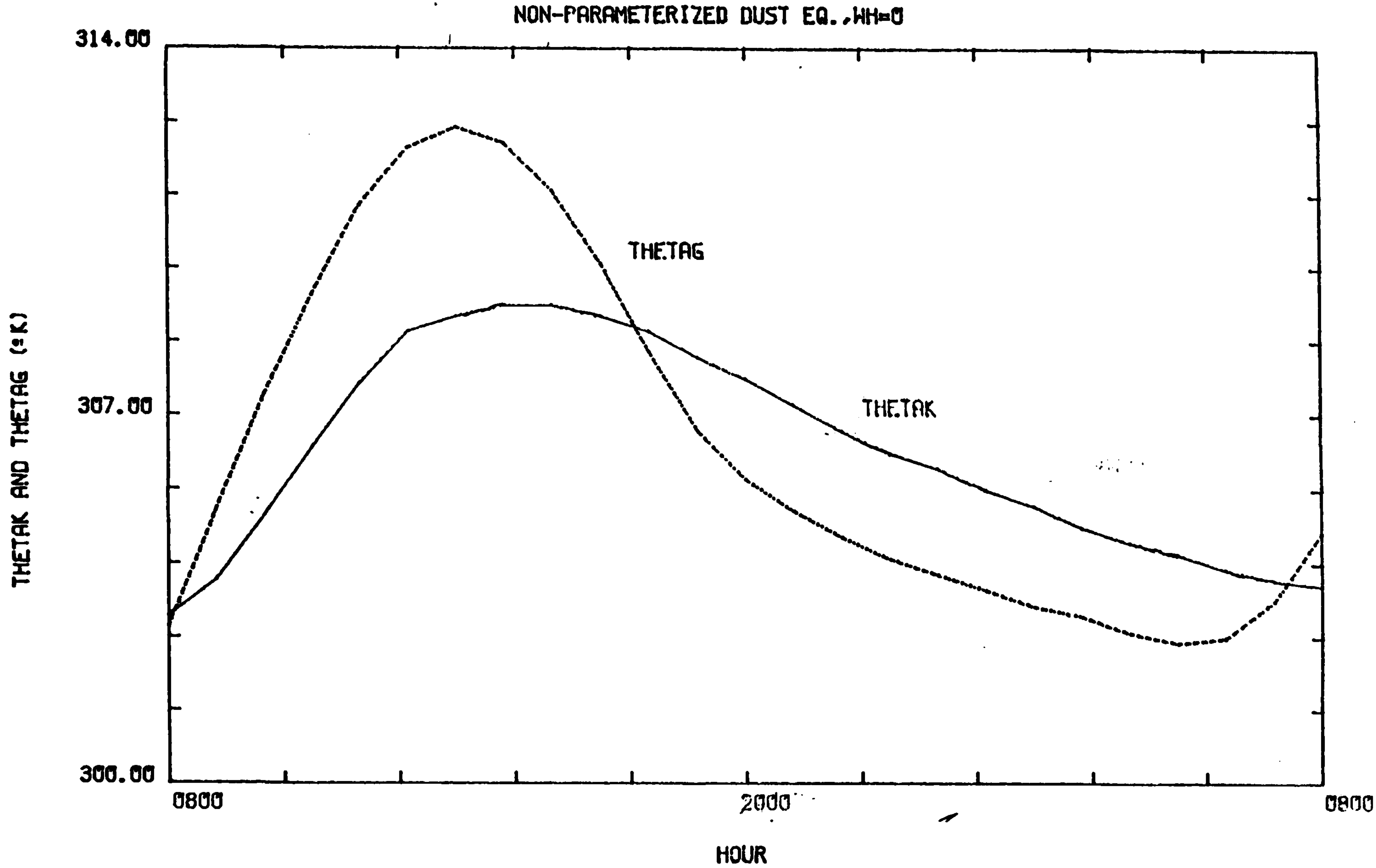

Fig. 5. - Same as Fig. 4 for θ_{Gr} and θ_k.

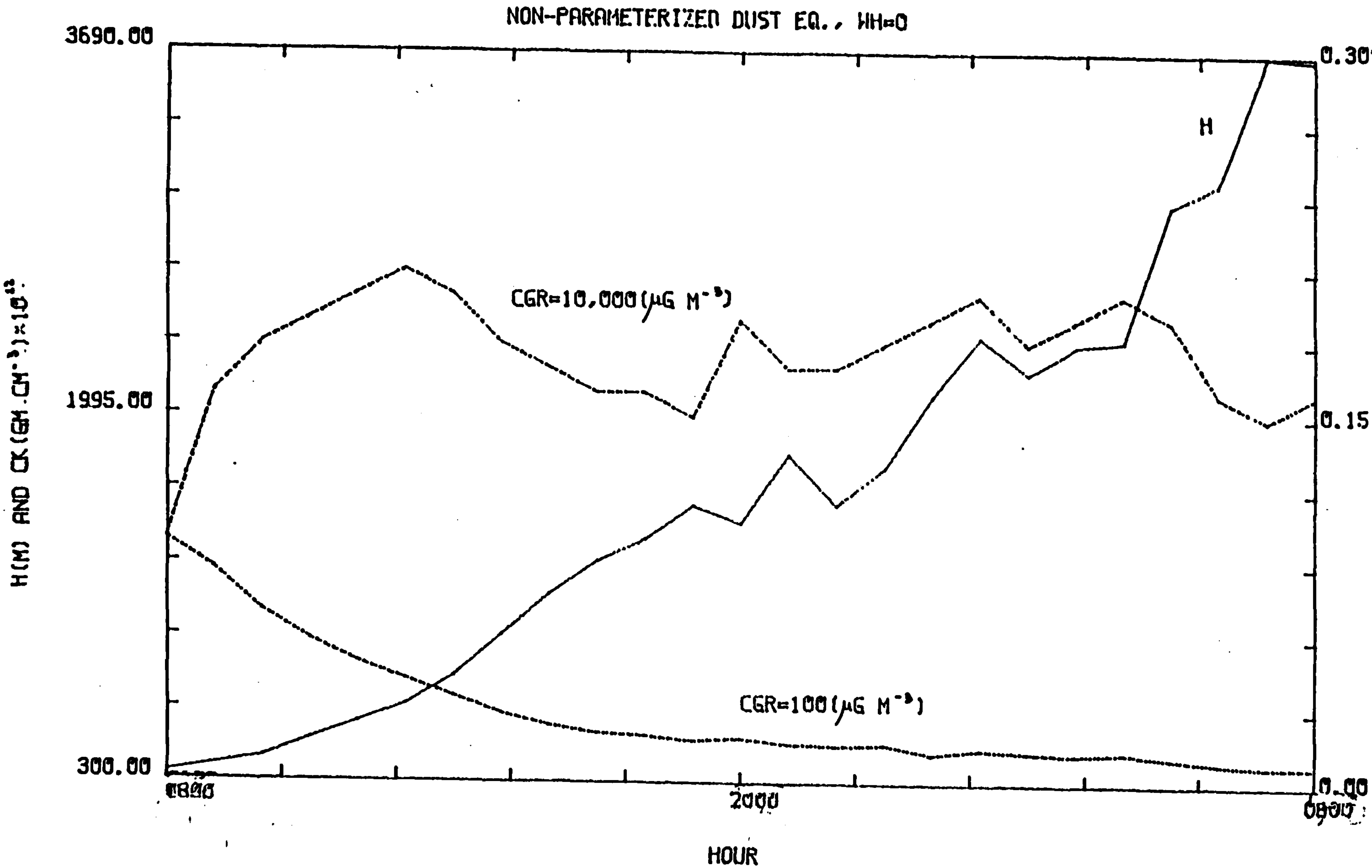

Fig. 6. - Same as Fig. 4 for h, C_k (for C_{gr} = 100 $\mu g\ m^{-3}$, 10,000 μgm^{-3}).

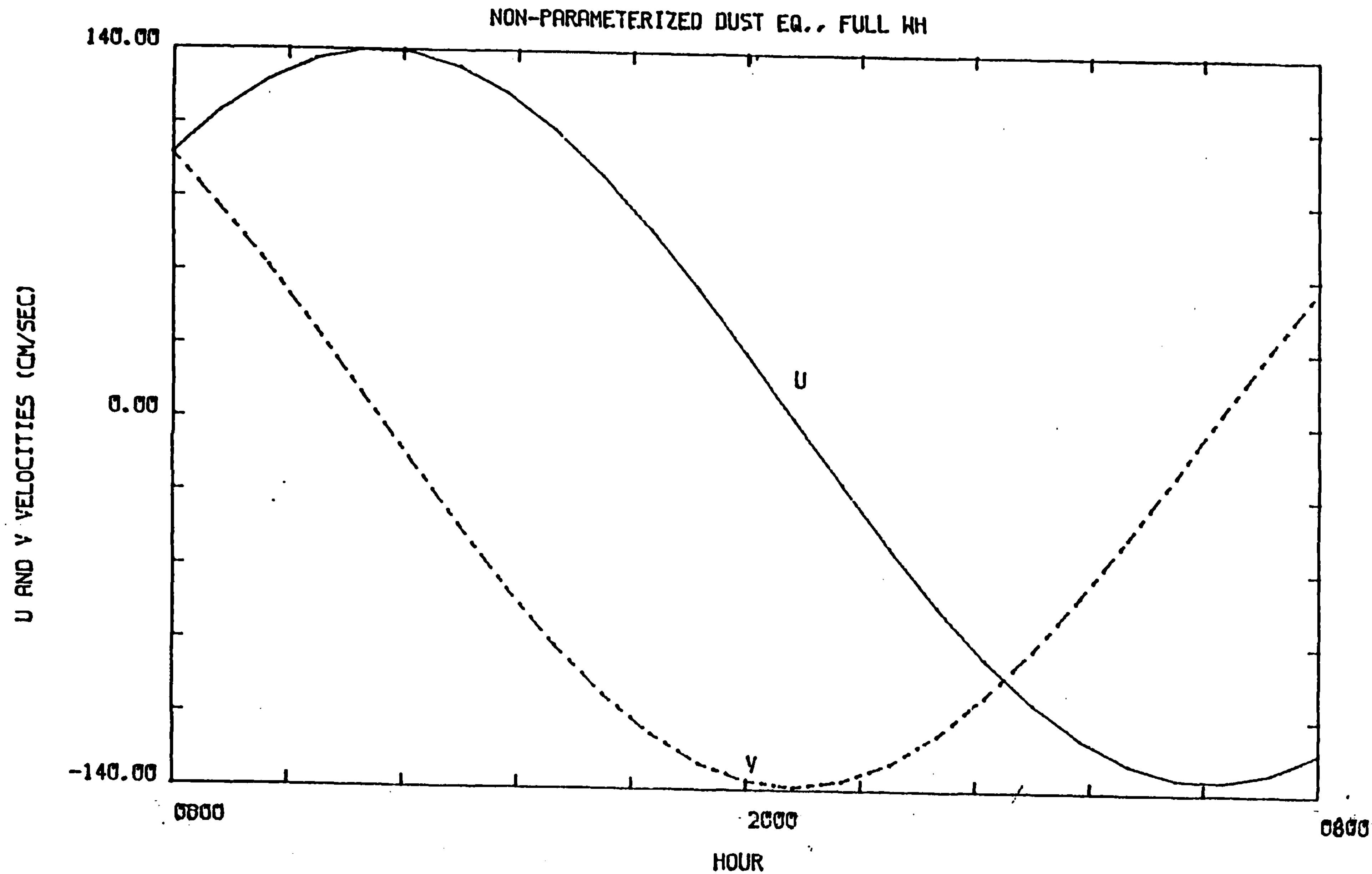

Fig. 7. – Same as Fig. 4 for $\hat{u}$, $\hat{v}$, $w_h \neq o$.

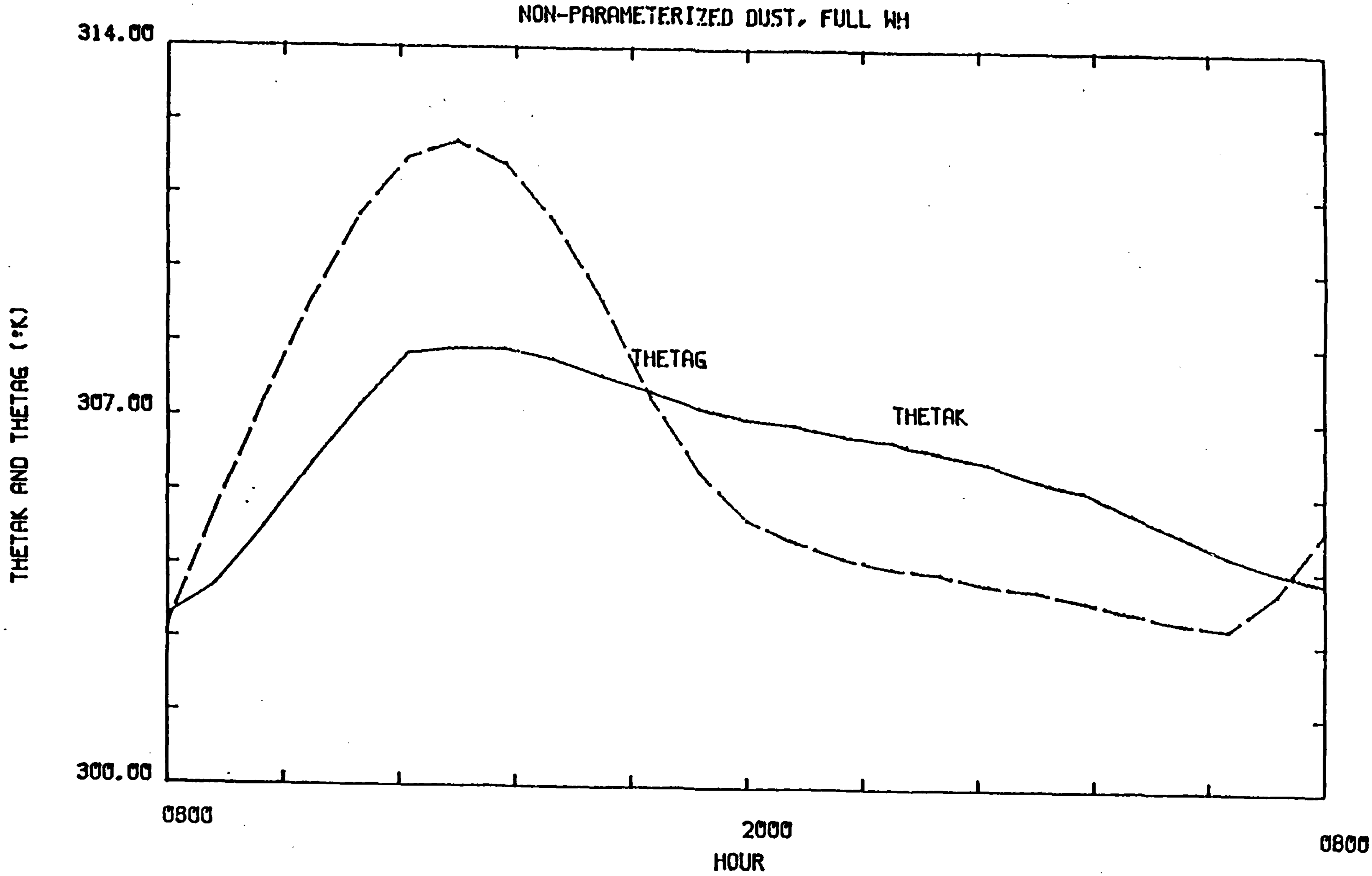

Fig. 8. - Same as Fig. 7 for θ_{GR} and θ_k.

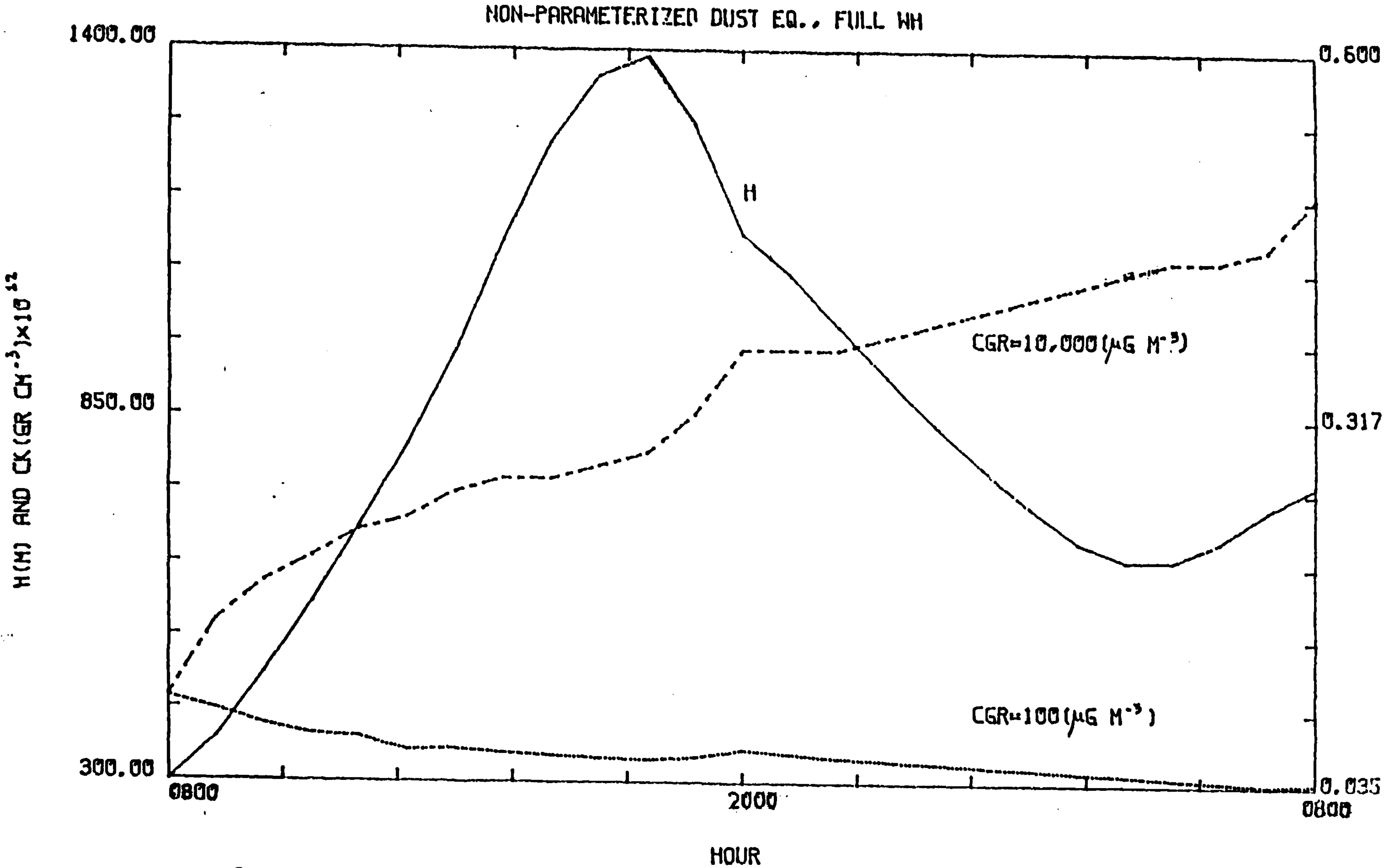

Fig. 9. - Same as Fig. 7 for h, C_k (for C_{gr} = 100 μgm^{-3}, 10,000 μgm^{-3}).

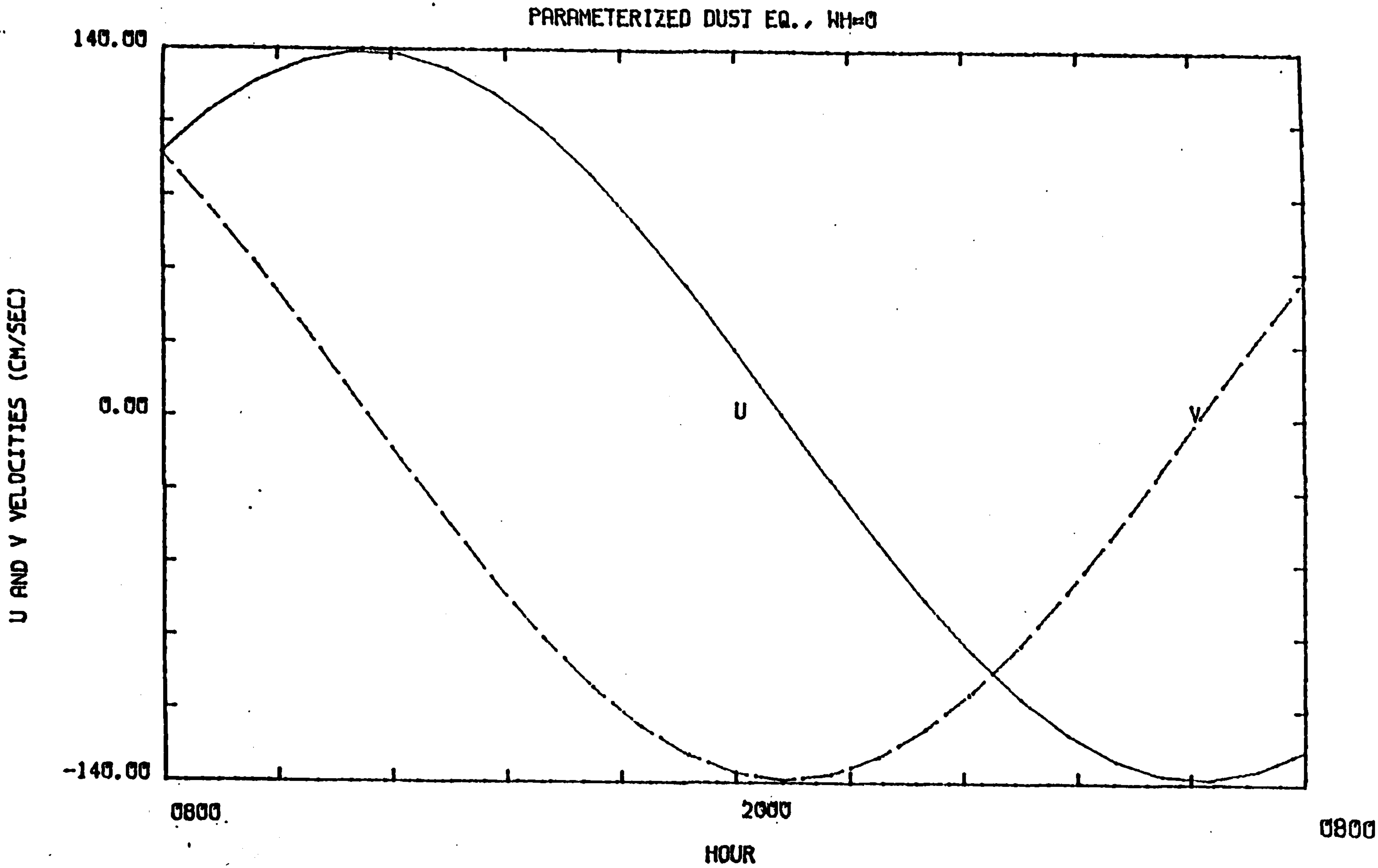

Fig. 10. - Evolution of $\hat{u}$ and $\hat{v}$ from One-Dimensional Parameterized Dust Model, $w_h = 0$.

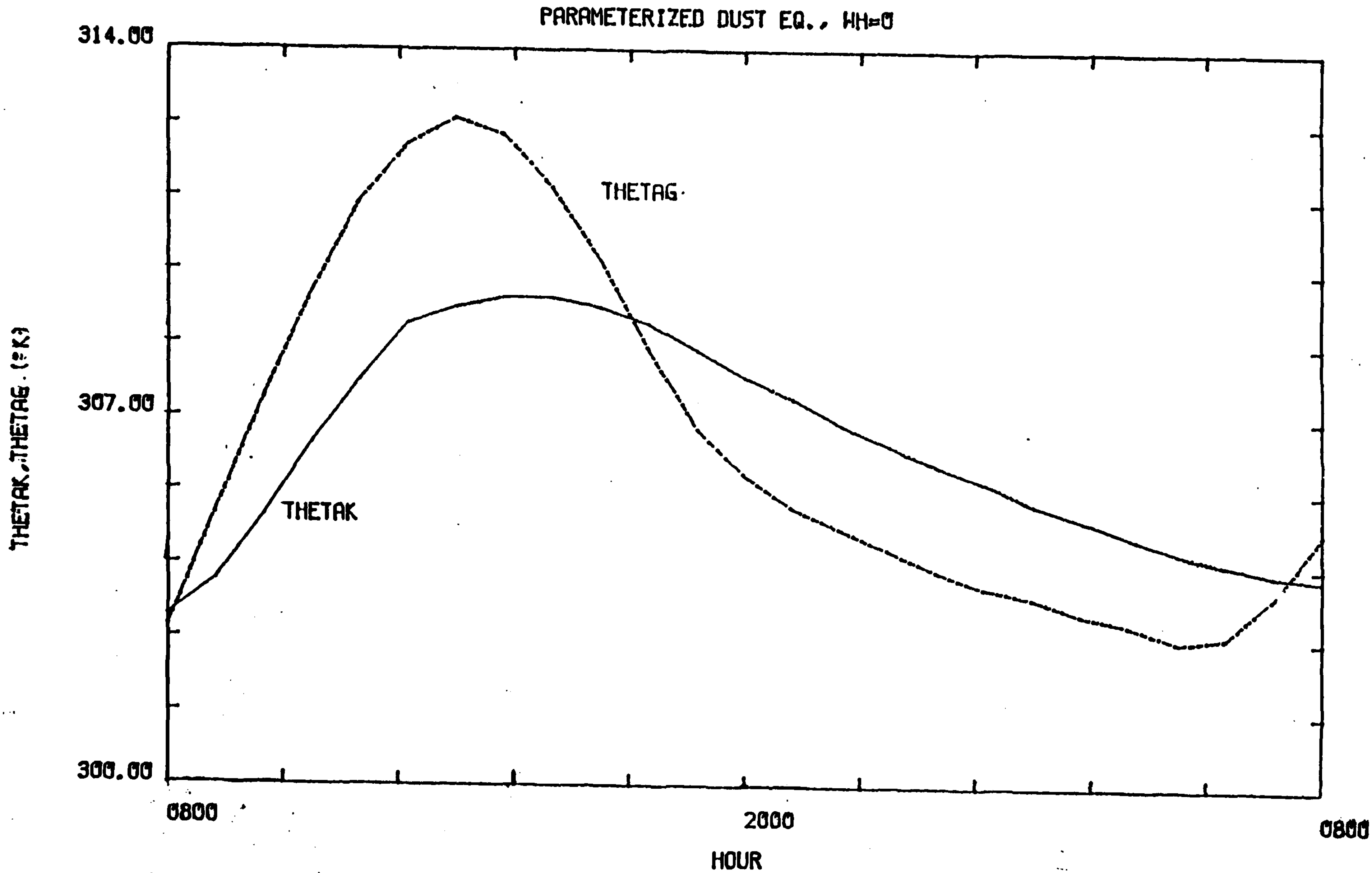

Fig. 11. - Same as Fig. 10 for θ_{GR} and θ_k.

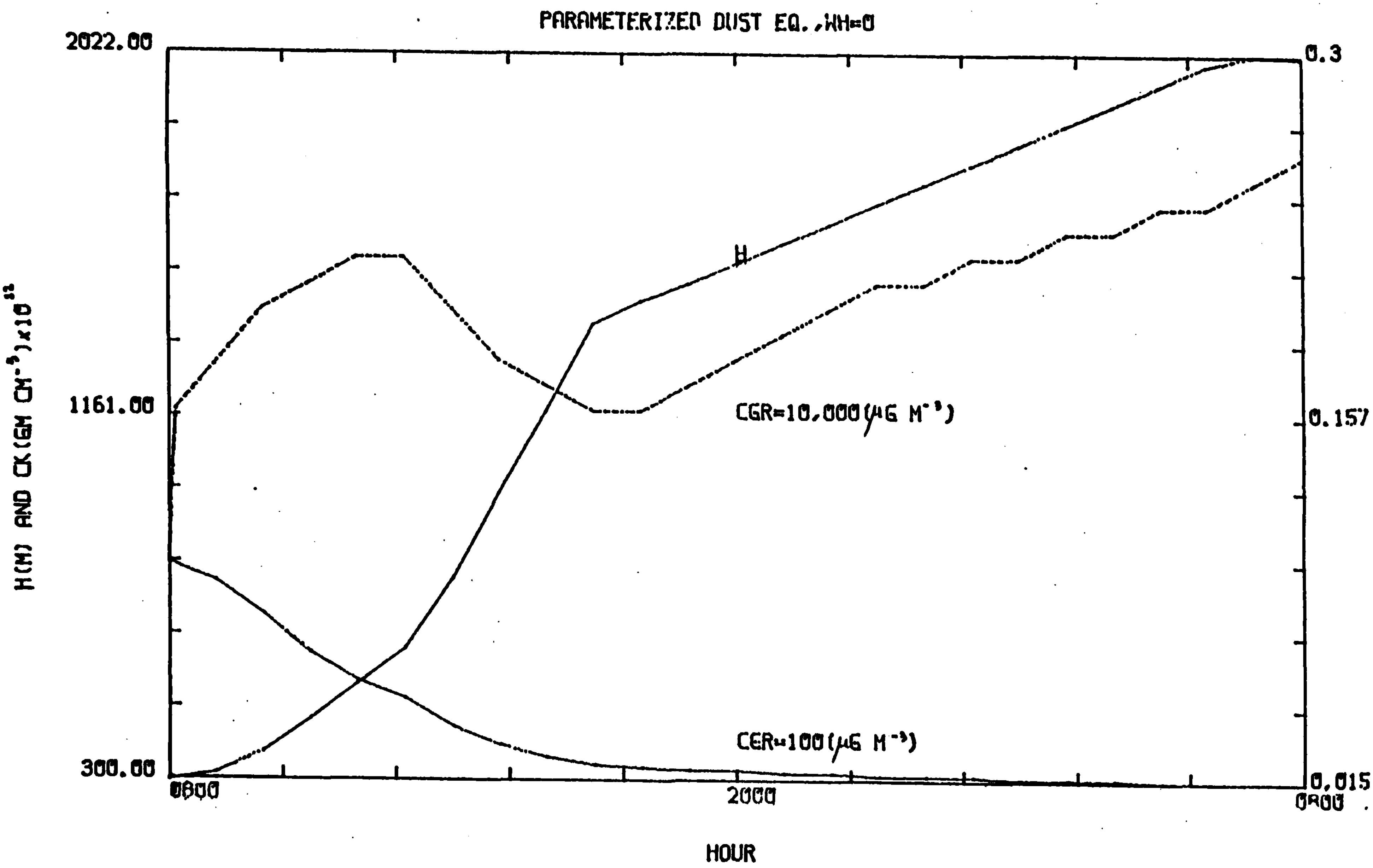

Fig. 12. - Same as Fig. 10 for h, C_k (C_{GR} = 100 μgm^{-3}, 10,000 μgm^{-3}).

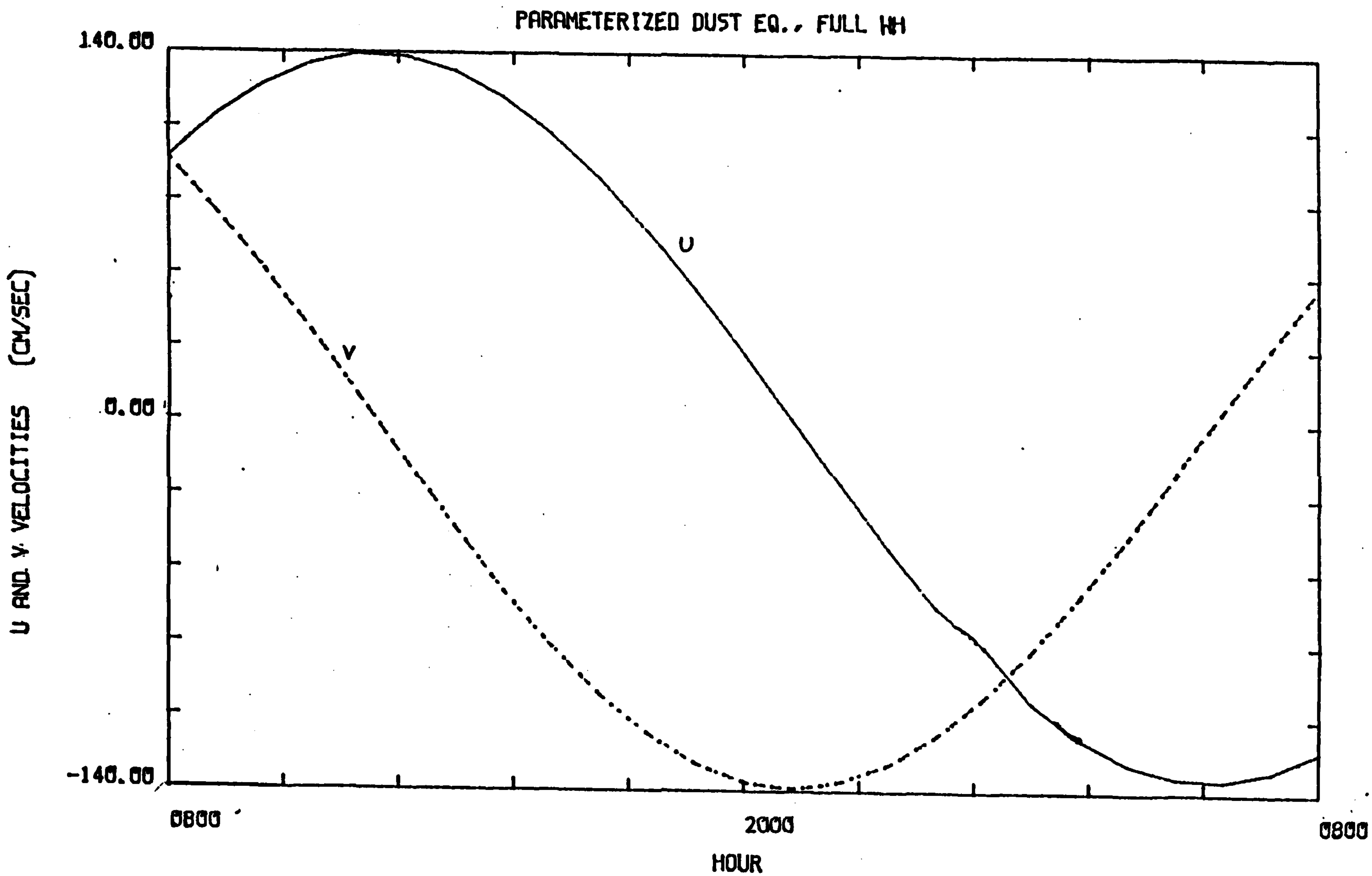

Fig. 13. - Same as Fig. 10 for $\hat{u}$, $\hat{v}$, $w_h \neq o$.

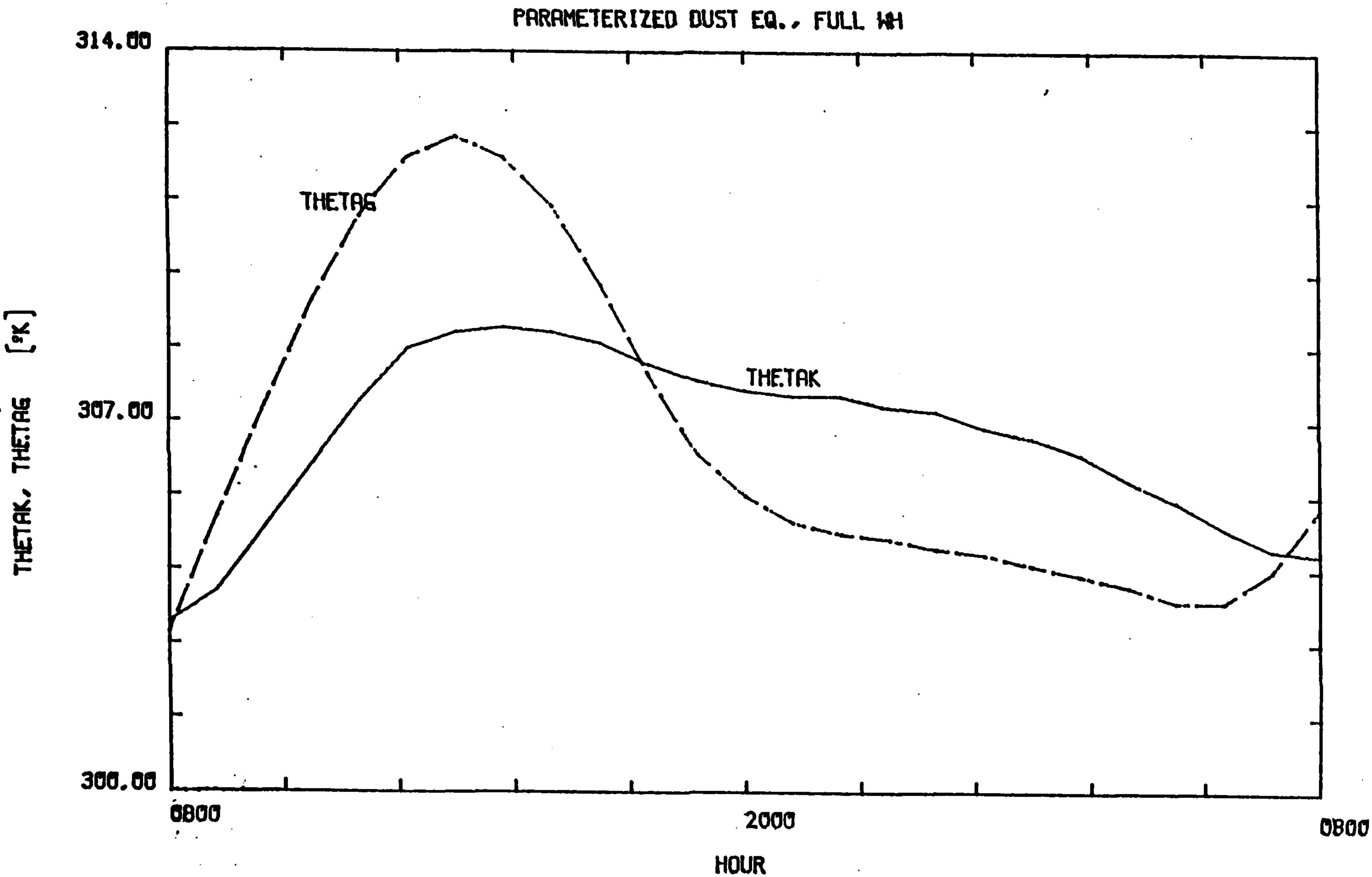

Fig. 14. – Same as Fig. 13 for θ_{GR} and θ_k.

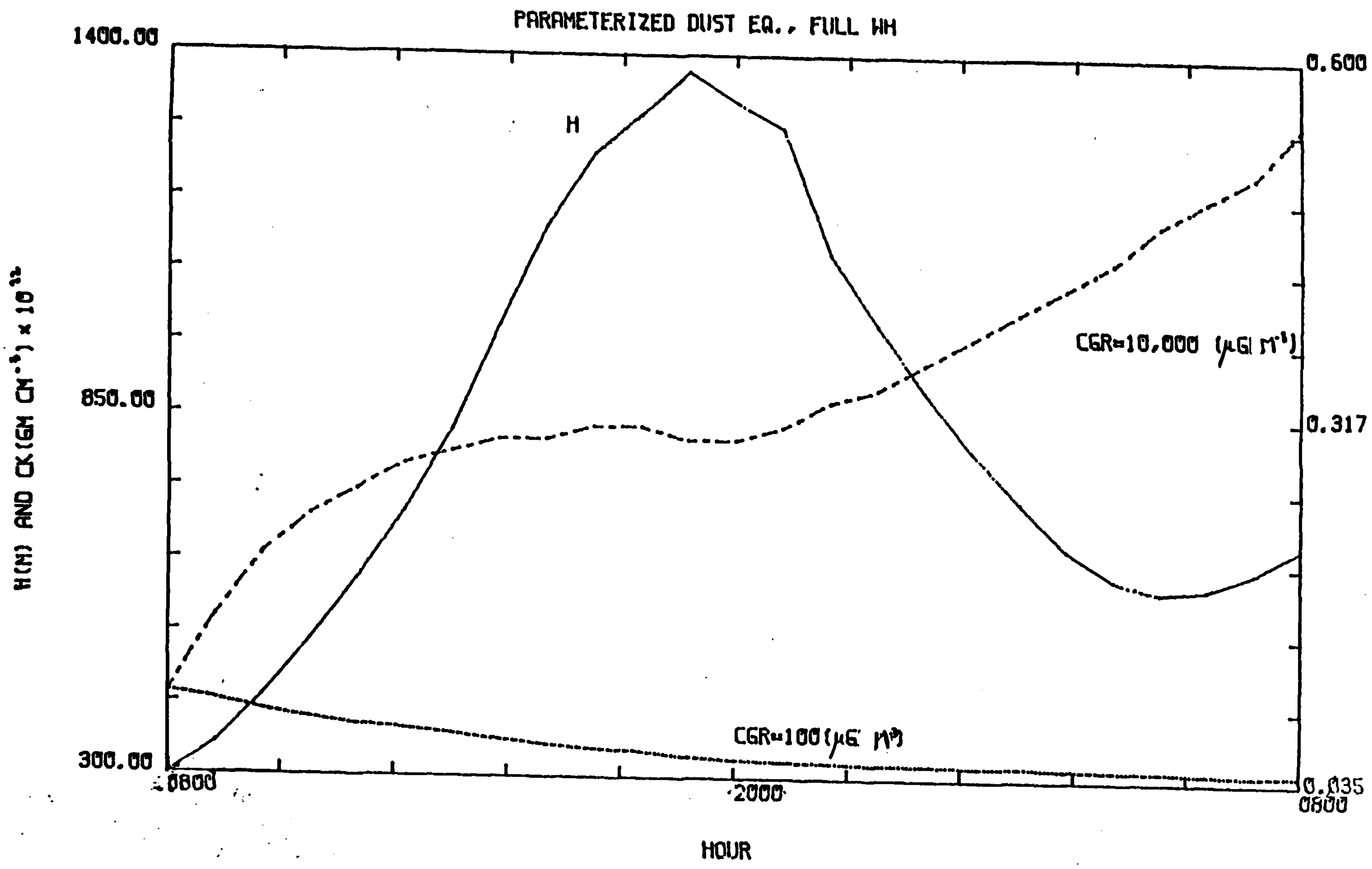

Fig. 15. – Same as Fig. 13 for h, C_k (C_{GR} = 100 μgm^{-3}, 10,000 μgm^{-3}).

U VELOCITY -FIELD IN CM/SEC STEP 180

J \ I	01	02	03	04 / 31	05 / 30	06 / 29	07 / 28	08 / 27	09 / 26	10 / 25	11 / 24	12 / 23	13 / 22	14 / 21	15 / 20	16 / 19	17 / 18
01	100	100	100	100	100	100	100	100	100	100	100	100	100	100	100	100	100
				100	100	100	100	100	100	100	100	100	100	100	100	100	100
02	100	93	98	97	97	97	97	97	97	97	97	97	97	97	97	97	97
				100	99	97	97	97	97	97	97	97	97	97	97	97	97
03	[illegible]	[illegible]	[illegible]	[illegible]	[illegible]	[illegible]	[illegible]	[illegible]	[illegible]	[illegible]	[illegible]	[illegible]	[illegible]	[illegible]	[illegible]	[illegible]	[illegible]
				[illegible]	[illegible]	[illegible]	[illegible]	[illegible]	[illegible]	[illegible]	[illegible]	[illegible]	[illegible]	[illegible]	[illegible]	[illegible]	[illegible]
04	[illegible]	[illegible]	[illegible]	[illegible]	[illegible]	[illegible]	[illegible]	[illegible]	[illegible]	[illegible]	[illegible]	[illegible]	[illegible]	[illegible]	[illegible]	[illegible]	[illegible]
				[illegible]	[illegible]	[illegible]	[illegible]	[illegible]	[illegible]	[illegible]	[illegible]	[illegible]	[illegible]	[illegible]	[illegible]	[illegible]	[illegible]
05	[illegible]	[illegible]	[illegible]	[illegible]	[illegible]	[illegible]	[illegible]	[illegible]	[illegible]	[illegible]	[illegible]	[illegible]	[illegible]	[illegible]	[illegible]	[illegible]	[illegible]
				100	[illegible]	[illegible]	[illegible]	[illegible]	[illegible]	[illegible]	[illegible]	[illegible]	[illegible]	[illegible]	[illegible]	[illegible]	[illegible]
58	100	[illegible]	[illegible]	[illegible]	[illegible]	[illegible]	[illegible]	[illegible]	[illegible]	[illegible]	[illegible]	[illegible]	[illegible]	[illegible]	[illegible]	[illegible]	[illegible]
				[illegible]	[illegible]	[illegible]	[illegible]	[illegible]	[illegible]	[illegible]	[illegible]	[illegible]	[illegible]	[illegible]	[illegible]	[illegible]	[illegible]
59	[illegible]	[illegible]	[illegible]	[illegible]	[illegible]	[illegible]	[illegible]	[illegible]	[illegible]	[illegible]	[illegible]	[illegible]	[illegible]	[illegible]	[illegible]	[illegible]	[illegible]
				[illegible]	[illegible]	[illegible]	[illegible]	[illegible]	[illegible]	[illegible]	[illegible]	[illegible]	[illegible]	[illegible]	[illegible]	[illegible]	[illegible]
60	[illegible]	[illegible]	[illegible]	[illegible]	[illegible]	[illegible]	[illegible]	[illegible]	[illegible]	[illegible]	[illegible]	[illegible]	[illegible]	[illegible]	[illegible]	[illegible]	[illegible]
				[illegible]	[illegible]	[illegible]	[illegible]	[illegible]	[illegible]	[illegible]	[illegible]	[illegible]	[illegible]	[illegible]	[illegible]	[illegible]	[illegible]
61	100	100	100	[illegible]	[illegible]	[illegible]	[illegible]	[illegible]	[illegible]	[illegible]	[illegible]	[illegible]	[illegible]	[illegible]	[illegible]	100	100
				100	100	100	100	100	100	100	100	100	100	100	100	100	100

Fig. 16. – $\hat{u}$ field at 180 minutes, constant B.C.

U VELOCITY -FIELD IN CM/SEC STEP 180

J \ I	01	02	03	04 / 31	05 / 30	06 / 29	07 / 28	08 / 27	09 / 26	10 / 25	11 / 24	12 / 23	13 / 22	14 / 21	15 / 20	16 / 19	17 / 18
01	[illegible]	[illegible]	[illegible]	[illegible]	[illegible]	[illegible]	[illegible]	[illegible]	[illegible]	[illegible]	[illegible]	[illegible]	96	96	96	96	96
				96	95	96	96	96	96	95	96	96	95	96	96	96	96
02	98	96	96	95	96	95	96	96	96	95	95	96	96	96	96	96	96
				96	96	96	96	96	96	95	96	96	96	96	96	96	96
03	[illegible]	[illegible]	[illegible]	[illegible]	[illegible]	[illegible]	[illegible]	[illegible]	[illegible]	[illegible]	[illegible]	[illegible]	[illegible]	[illegible]	[illegible]	[illegible]	[illegible]
				[illegible]	[illegible]	[illegible]	[illegible]	[illegible]	[illegible]	[illegible]	[illegible]	[illegible]	[illegible]	[illegible]	[illegible]	[illegible]	[illegible]
04	[illegible]	[illegible]	[illegible]	[illegible]	[illegible]	[illegible]	[illegible]	[illegible]	[illegible]	[illegible]	[illegible]	[illegible]	[illegible]	[illegible]	[illegible]	[illegible]	[illegible]
				[illegible]	[illegible]	[illegible]	[illegible]	[illegible]	[illegible]	[illegible]	[illegible]	[illegible]	[illegible]	[illegible]	[illegible]	[illegible]	[illegible]
05	[illegible]	[illegible]	[illegible]	[illegible]	[illegible]	[illegible]	[illegible]	[illegible]	[illegible]	[illegible]	[illegible]	[illegible]	[illegible]	[illegible]	[illegible]	[illegible]	[illegible]
				96	96	96	96	96	96	95	95	96	96	96	96	96	96
58	99	96	95	96	95	95	96	95	96	95	95	96	96	95	96	96	96
				95	95	96	96	96	95	95	96	96	96	96	96	96	96
59	[illegible]	[illegible]	[illegible]	[illegible]	[illegible]	[illegible]	[illegible]	[illegible]	[illegible]	[illegible]	[illegible]	[illegible]	[illegible]	[illegible]	[illegible]	[illegible]	[illegible]
				[illegible]	[illegible]	[illegible]	[illegible]	[illegible]	[illegible]	[illegible]	[illegible]	[illegible]	[illegible]	[illegible]	[illegible]	[illegible]	[illegible]
60	[illegible]	[illegible]	[illegible]	[illegible]	[illegible]	[illegible]	[illegible]	[illegible]	[illegible]	[illegible]	[illegible]	[illegible]	[illegible]	[illegible]	[illegible]	[illegible]	[illegible]
				[illegible]	[illegible]	[illegible]	[illegible]	[illegible]	[illegible]	[illegible]	[illegible]	[illegible]	[illegible]	[illegible]	[illegible]	[illegible]	[illegible]
61	[illegible]	100	[illegible]	[illegible]	[illegible]	[illegible]	[illegible]	[illegible]	[illegible]	[illegible]	[illegible]	[illegible]	[illegible]	[illegible]	104	102	98
				91	103	97	119	101	108	104	95	95	102	100	105	109	96

Fig. 17. – $\hat{u}$ field at 180 minutes, radiation B.C.

V VELOCITY -FIELD IN *.1 CM/SEC STEP 130

I:	01	02	03	04	05	06	07	08	09	10	11	12	13	14	15	16	17
				31	30	29	28	27	26	25	24	23	22	21	20	19	18
J: 01	0	0	0	0	0	0	0	0	0	0	0	0	0	0	0	0	0
				0	0	0	0	0	0	0	0	0	0	0	0	0	0
02	0	-40	-41	-41	-41	-41	-41	-41	-41	-41	-41	-41	-41	-41	-41	-41	-41
				0	-59	-41	-41	-41	-41	-41	-41	-41	-41	-41	-41	-41	-41
03	0	-75	-75	-75	-75	-75	-75	-75	-75	-75	-75	-75	-75	-75	-75	-75	-75
				0	-76	-75	-75	-75	-75	-75	-75	-75	-75	-75	-75	-75	-75
04	0	-77	-77	-77	-77	-77	-77	-77	-77	-77	-77	-77	-77	-77	-77	-77	-77
				[illegible]	-77	-77	-77	-77	-77	-77	-77	-77	-77	-77	-77	-77	-77
05	0	-78	-78	[illegible]	[illegible]	[illegible]	[illegible]	[illegible]	[illegible]	[illegible]	[illegible]	[illegible]	-78	-78	-78	-78	-78
				[illegible]	[illegible]	[illegible]	[illegible]	-78	-78	-78	-78	-78	-78	-78	-78	-78	-78
58	0	-77	-77	[illegible]	[illegible]	[illegible]	[illegible]	[illegible]	-78	-78	-78	-78	-78	-78	-78	-78	-78
				[illegible]	-77	-77	[illegible]	-77	-78	-78	-78	-78	-78	-78	-78	-78	-78
59	0	-77	-77	-77	-77	-77	-77	-77	-77	-77	-77	-77	-77	-77	-77	-77	-77
				[illegible]	-77	-77	-77	-77	-77	-77	-77	-77	-77	-77	-77	-77	-77
60	0	-33	-67	[illegible]	-67	-67	-67	-67	-67	-67	-67	-67	-57	-57	-67	-67	-57
				[illegible]	-71	-67	-67	-67	-67	-67	-67	-57	-67	-57	-57	-57	-67
61	0	0	0	0	0	0	0	0	0	0	0	0	0	0	0	0	0
				0	0	0	0	0	0	0	0	0	0	0	0	0	0

Fig. 18. – $\hat{v}$ field at 180 minutes, constant B.C.

V VELOCITY -FIELD IN *.1 CM/SEC STEP 180

I:	01	02	03	04	05	06	07	08	09	10	11	12	13	14	15	16	17
				31	30	29	28	27	26	25	24	23	22	21	20	19	18
J: 01	-174	-32	-37	[illegible]	[illegible]	[illegible]	[illegible]	-104	-37	-43	-101	-94	-95	-116	-96	-46	-66
				[illegible]	[illegible]	[illegible]	[illegible]	[illegible]	-72	-72	-62	[illegible]	-92	[illegible]	-80	[illegible]	-36
02	-75	-75	-75	[illegible]	[illegible]	[illegible]	[illegible]	[illegible]	[illegible]	-78	-78	-75	-76	-78	-76	-76	-76
				-79	-78	-78	-78	-78	-78	-78	-78	-78	-78	-78	-78	-73	-78
03	-79	-78	-78	-78	-78	-78	-78	-78	-78	-79	-78	-73	-78	-78	-78	-78	-78
				[illegible]	-78	-79	-76	-78	-78	-79	-79	-79	-73	-78	-78	-78	-78
04	-79	-77	[illegible]	[illegible]	[illegible]	[illegible]	[illegible]	[illegible]	[illegible]	[illegible]	-78	[illegible]	-73	-73	[illegible]	-78	-76
				[illegible]	[illegible]	[illegible]	[illegible]	[illegible]	[illegible]	[illegible]	[illegible]	[illegible]	-73	-73	[illegible]	-76	-73
05	[illegible]	[illegible]	[illegible]	[illegible]	[illegible]	[illegible]	[illegible]	[illegible]	[illegible]	[illegible]	[illegible]	[illegible]	-73	-78	-78	-73	-78
				[illegible]	[illegible]	[illegible]	[illegible]	[illegible]	[illegible]	[illegible]	[illegible]	[illegible]	[illegible]	-78	-78	-73	-78
58	-79	-79	-78	[illegible]	[illegible]	[illegible]	[illegible]	[illegible]	[illegible]	[illegible]	-78	[illegible]	-78	-78	-78	-78	-78
				-75	-78	-78	-78	-78	-79	-79	-78	-78	-78	-78	-78	-78	-78
59	-79	-77	-78	-78	-78	-78	-78	-78	-72	-79	-78	-78	-78	-73	-78	-76	-78
				-75	-78	-78	-78	-78	-72	-73	-78	-78	-78	-78	-78	-78	-78
60	-79	-78	[illegible]	[illegible]	[illegible]	[illegible]	[illegible]	[illegible]	[illegible]	-79	-78	-78	-78	-79	-78	-73	-78
				[illegible]	[illegible]	[illegible]	[illegible]	[illegible]	[illegible]	[illegible]	-78	-78	-78	-78	-78	-73	-78
61	-79	-78	-80	[illegible]	[illegible]	[illegible]	[illegible]	[illegible]	-76	-79	-79	-79	-79	-80	-80	-80	-80
				[illegible]	[illegible]	[illegible]	[illegible]	-80	[illegible]	[illegible]	-80	-80	-80	-80	-80	-80	-80

Fig. 19. – $\hat{v}$ field at 180 minutes, radiation B.C.

~~BL HEIGHT -FIELD IN METERS STEP [illegible]~~

J \ I:	01	02	03	04 / 31	05 / 30	06 / 29	07 / 28	08 / 27	09 / 26	10 / 25	11 / 24	12 / 23	13 / 22	14 / 21	15 / 20	16 / 19	17 / 18
01	650	650	650	[illegible]	[illegible]	[illegible]	[illegible]	[illegible]	[illegible]	[illegible]	650	650	650	650	650	650	650
02	650	702	[illegible]	[illegible]	[illegible]	[illegible]	[illegible]	[illegible]	[illegible]	[illegible]	[illegible]	[illegible]	[illegible]	[illegible]	[illegible]	[illegible]	[illegible]
03	650	701	710	[illegible]	710	711	710	710	710	710	710	710	710	710	710	710	710
				650	675	717	715	703	711	710	710	710	710	710	710	710	710
04	650	698	714	713	714	714	714	714	714	714	714	714	714	714	714	714	714
				650	683	715	714	714	714	713	714	714	714	714	714	714	714
05	650	699	717	[illegible]	[illegible]	[illegible]	[illegible]	[illegible]	[illegible]	[illegible]	[illegible]	[illegible]	[illegible]	[illegible]	[illegible]	[illegible]	[illegible]
06	650	701	717	[illegible]	[illegible]	[illegible]	[illegible]	[illegible]	[illegible]	[illegible]	[illegible]	[illegible]	[illegible]	[illegible]	[illegible]	[illegible]	[illegible]
59	650	702	721	[illegible]	[illegible]	[illegible]	[illegible]	[illegible]	[illegible]	[illegible]	[illegible]	[illegible]	[illegible]	[illegible]	[illegible]	727	727
				[illegible]	[illegible]	727	727	727	727	727	727	727	727	727	727	727	727
60	650	673	687	[illegible]	701	691	691	691	691	691	691	691	691	691	691	691	691
				650	675	[illegible]	[illegible]	691	691	691	691	691	691	691	691	691	691
61	[illegible]	[illegible]	[illegible]	[illegible]	[illegible]	[illegible]	[illegible]	[illegible]	[illegible]	[illegible]	[illegible]	[illegible]	[illegible]	[illegible]	[illegible]	[illegible]	[illegible]

Fig. 20. - Inversion height at 180 minutes, constant B.C.

~~BL HEIGHT -FIELD IN METERS STEP [illegible]~~

J \ I:	01	02	03	04 / 31	05 / 30	06 / 29	07 / 28	08 / 27	09 / 26	10 / 25	11 / 24	12 / 23	13 / 22	14 / 21	15 / 20	16 / 19	17 / 18
01	711	707	[illegible]	[illegible]	[illegible]	747	[illegible]	[illegible]	716	[illegible]	733	739	729	653	763	660	660
02	714	713	[illegible]	[illegible]	[illegible]	[illegible]	[illegible]	[illegible]	[illegible]	[illegible]	[illegible]	[illegible]	719	719	719	[illegible]	[illegible]
03	683	717	718	[illegible]	[illegible]	[illegible]	[illegible]	[illegible]	[illegible]	[illegible]	[illegible]	718	718	718	718	718	718
				719	719	718	718	718	718	717	718	718	717	718	717	718	719
04	704	717	718	719	719	719	719	719	719	719	719	718	719	719	718	719	719
				719	719	719	719	719	719	719	718	719	719	718	719	718	718
05	705	717	[illegible]	[illegible]	[illegible]	[illegible]	[illegible]	[illegible]	[illegible]	[illegible]	[illegible]	[illegible]	[illegible]	[illegible]	[illegible]	[illegible]	[illegible]
[illegible]	[illegible]	[illegible]	[illegible]	[illegible]	[illegible]	[illegible]	[illegible]	[illegible]	[illegible]	[illegible]	[illegible]	[illegible]	[illegible]	[illegible]	[illegible]	[illegible]	[illegible]
59	519	718	718	[illegible]	[illegible]	[illegible]	[illegible]	[illegible]	[illegible]	[illegible]	[illegible]	[illegible]	[illegible]	718	718	718	718
				713	719	719	719	718	718	718	713	718	718	718	718	718	718
60	755	717	719	718	719	719	719	719	719	719	719	718	718	718	718	719	719
				719	719	719	719	718	718	718	718	719	719	719	719	718	718
61	715	719	719	[illegible]	[illegible]	[illegible]	[illegible]	[illegible]	[illegible]	[illegible]	[illegible]	[illegible]	719	719	719	719	719

Fig. 21. - Inversion height at 180 minutes, radiation B.C.

J	01	02	03	31	30	29	28	27	26	25	24	23	22	21	20	19	18
01	303	303	303	303	303	303	303	303	303	303	303	303	303	303	303	303	303
				303	303	303	303	303	303	303	303	303	303	303	303	303	303
02	303	312	312	311	311	311	311	311	311	311	311	311	311	311	311	311	311
				303	315	314	312	311	311	311	311	311	311	311	311	311	311
03	[illegible]	[illegible]	[illegible]	[illegible]	[illegible]	[illegible]	[illegible]	[illegible]	[illegible]	[illegible]	[illegible]	[illegible]	[illegible]	[illegible]	[illegible]	[illegible]	[illegible]
04	[illegible]	[illegible]	[illegible]	[illegible]	[illegible]	[illegible]	[illegible]	[illegible]	[illegible]	[illegible]	[illegible]	[illegible]	[illegible]	[illegible]	[illegible]	[illegible]	[illegible]
05	303	309	300	302	307	309	[illegible]	[illegible]	[illegible]	307	[illegible]	[illegible]	308	308	308	308	308
59	303	314	312	[illegible]	[illegible]	[illegible]	[illegible]	[illegible]	[illegible]	[illegible]	[illegible]	[illegible]	313	313	313	313	313
				[illegible]	[illegible]	315	312	313	[illegible]	[illegible]	313	313	313	313	313	313	313
60	303	305	[illegible]	304	304	304	304	304	304	304	304	304	304	304	304	304	304
61	[illegible]	[illegible]	[illegible]	[illegible]	[illegible]	[illegible]	[illegible]	[illegible]	[illegible]	[illegible]	[illegible]	[illegible]	[illegible]	[illegible]	[illegible]	[illegible]	[illegible]

Fig. 22. – θ_K at 180 minutes, constant B.C.

J	01	02	03	31	30	29	28	27	26	25	24	23	22	21	20	19	18
01	309	306	307	303	307	307	307	307	307	307	307	307	307	307	307	307	307
				306	307	307	306	306	307	307	307	307	309	308	307	307	307
02	307	[illegible]	[illegible]	[illegible]	[illegible]	[illegible]	[illegible]	[illegible]	[illegible]	[illegible]	[illegible]	[illegible]	[illegible]	[illegible]	[illegible]	[illegible]	[illegible]
03	[illegible]	307	[illegible]	[illegible]	[illegible]	[illegible]	[illegible]	[illegible]	[illegible]	[illegible]	[illegible]	[illegible]	[illegible]	[illegible]	[illegible]	[illegible]	[illegible]
04	307	307	307	[illegible]	[illegible]	[illegible]	[illegible]	[illegible]	[illegible]	[illegible]	[illegible]	[illegible]	[illegible]	[illegible]	[illegible]	[illegible]	[illegible]
05	307	307	307	306	307	307	307	307	[illegible]	[illegible]	308	308	308	308	308	305	308
				[illegible]	307	307	307	307	[illegible]	[illegible]	303	[illegible]	308	308	308	303	303
59	307	307	308	305	309	307	307	307	308	307	309	308	309	308	308	308	308
				310	307	307	307	303	303	303	308	308	307	307	307	307	308
60	307	307	307	307	307	307	307	307	307	307	307	307	307	307	307	307	307
61	[illegible]	[illegible]	[illegible]	[illegible]	[illegible]	[illegible]	[illegible]	[illegible]	[illegible]	[illegible]	[illegible]	[illegible]	[illegible]	315	339	308	[illegible]	[illegible]

Fig. 23. – θ_K at 180 minutes, radiation B.C.

J \ I	01	02	03	04	05	06	07	08	09	10	11	12	13	14	15	16	17
01	303	303	303	303	303	303	303	303	303	303	303	303	303	303	303	303	303
02	303	308	309	309	309	309	309	309	309	309	309	309	309	309	309	309	309
03	[illegible]	[illegible]	[illegible]	[illegible]	[illegible]	[illegible]	[illegible]	[illegible]	[illegible]	[illegible]	[illegible]	[illegible]	[illegible]	[illegible]	[illegible]	[illegible]	[illegible]
04	[illegible]	[illegible]	[illegible]	[illegible]	[illegible]	[illegible]	[illegible]	[illegible]	[illegible]	[illegible]	[illegible]	[illegible]	[illegible]	[illegible]	[illegible]	[illegible]	[illegible]
05	303	309	311	311	311	311	311	311	311	311	311	311	311	311	311	311	311
58	303	309	31[illegible]	311	311	311	311	311	311	311	311	311	311	311	311	311	311
59	[illegible]	[illegible]	[illegible]	[illegible]	[illegible]	[illegible]	[illegible]	[illegible]	[illegible]	[illegible]	[illegible]	[illegible]	[illegible]	[illegible]	[illegible]	[illegible]	[illegible]
60	303	312	[illegible]	[illegible]	[illegible]	[illegible]	[illegible]	[illegible]	[illegible]	[illegible]	[illegible]	[illegible]	[illegible]	[illegible]	[illegible]	[illegible]	[illegible]
61	303	303	303	303	303	303	303	303	303	303	303	303	303	303	303	303	303

Fig. 24. - θ_{GR} at 180 minutes, constant B.C.

J \ I	01	02	03	04	05	06	07	08	09	10	11	12	13	14	15	16	17
01	311	311	311	311	311	311	311	311	311	311	311	311	311	311	311	311	311
02	311	311	311	311	311	311	311	311	311	311	311	311	311	311	311	311	311
03	[illegible]	[illegible]	[illegible]	[illegible]	[illegible]	[illegible]	[illegible]	[illegible]	[illegible]	[illegible]	[illegible]	[illegible]	[illegible]	[illegible]	[illegible]	[illegible]	[illegible]
04	[illegible]	[illegible]	[illegible]	[illegible]	[illegible]	[illegible]	[illegible]	[illegible]	[illegible]	[illegible]	[illegible]	[illegible]	[illegible]	[illegible]	[illegible]	[illegible]	[illegible]
05	311	311	311	311	311	311	311	311	311	311	311	311	311	311	311	311	311
58	311	311	311	311	311	311	311	311	311	311	311	311	311	311	311	311	311
59	[illegible]	[illegible]	[illegible]	[illegible]	[illegible]	[illegible]	[illegible]	[illegible]	[illegible]	[illegible]	[illegible]	[illegible]	[illegible]	[illegible]	[illegible]	[illegible]	[illegible]
60	[illegible]	[illegible]	[illegible]	[illegible]	[illegible]	[illegible]	[illegible]	[illegible]	[illegible]	[illegible]	[illegible]	[illegible]	[illegible]	[illegible]	[illegible]	[illegible]	[illegible]
61	311	305	310	311	311	307	311	311	311	311	311	311	311	306	311	311	309
				309	307	311	311	310	311	311	311	311	311	311	306	311	311

Fig. 25. - θ_{GR} at 180 minutes, radiation B.C.

DUST CONC -FIELD IN *10 UG/M3 STEP 180

I	01	02	03	04	05	06	07	08	09	10	11	12	13	14	15	16	17
J				31	30	29	28	27	26	25	24	23	22	21	20	19	18
01	10	10	10	[illegible]	[illegible]	[illegible]	[illegible]	[illegible]	[illegible]	[illegible]	[illegible]	10	10	10	10	10	10
				10	10	10	10	10	10	10	10	10	10	10	10	10	10
02	10	18	19	19	19	19	19	19	19	19	19	19	19	19	19	19	19
				10	23	19	19	19	19	19	19	19	19	19	19	19	19
03	10	17	19	19	19	19	19	19	19	19	19	19	19	19	19	19	19
				[illegible]	[illegible]	[illegible]	[illegible]	[illegible]	19	19	19	19	19	19	19	19	19
04	10	17	[illegible]	[illegible]	[illegible]	[illegible]	[illegible]	[illegible]	[illegible]	[illegible]	[illegible]	[illegible]	[illegible]	[illegible]	[illegible]	[illegible]	[illegible]
				[illegible]	[illegible]	[illegible]	[illegible]	[illegible]	[illegible]	19	19	19	19	19	19	19	19
05	10	17	[illegible]	[illegible]	[illegible]	[illegible]	[illegible]	[illegible]	[illegible]	[illegible]	[illegible]	[illegible]	[illegible]	[illegible]	[illegible]	[illegible]	[illegible]
				[illegible]	[illegible]	[illegible]	[illegible]	[illegible]	[illegible]	[illegible]	[illegible]	[illegible]	[illegible]	[illegible]	[illegible]	[illegible]	[illegible]
53	10	17	19	[illegible]	[illegible]	[illegible]	[illegible]	[illegible]	[illegible]	[illegible]	[illegible]	[illegible]	[illegible]	19	19	[illegible]	19
				[illegible]	[illegible]	[illegible]	[illegible]	[illegible]	[illegible]	[illegible]	[illegible]	[illegible]	[illegible]	19	19	[illegible]	19
59	10	[illegible]	[illegible]	[illegible]	[illegible]	[illegible]	[illegible]	[illegible]	[illegible]	[illegible]	[illegible]	[illegible]	10	10	[illegible]	[illegible]	19
				[illegible]	[illegible]	[illegible]	[illegible]	[illegible]	[illegible]	[illegible]	[illegible]	[illegible]	[illegible]	[illegible]	[illegible]	[illegible]	[illegible]
60	10	[illegible]	19	[illegible]	[illegible]	[illegible]	[illegible]	[illegible]	[illegible]	[illegible]	[illegible]	[illegible]	[illegible]	[illegible]	[illegible]	[illegible]	[illegible]
				[illegible]	21	[illegible]	[illegible]	[illegible]	[illegible]	[illegible]	[illegible]	[illegible]	[illegible]	[illegible]	[illegible]	19	19
61	10	10	10	[illegible]	[illegible]	[illegible]	[illegible]	[illegible]	[illegible]	[illegible]	[illegible]	[illegible]	[illegible]	[illegible]	10	10	10
				[illegible]	10	10	[illegible]	[illegible]	[illegible]	[illegible]	10	10	10	13	10	10	10

Fig. 26. - C_k at 180 minutes, constant B.C.

DUST CONC -FIELD IN *10 UG/M3 STEP 180

I	01	02	03	04	05	06	07	08	09	10	11	12	13	14	15	16	17
J				31	30	29	28	27	26	25	24	23	22	21	20	19	18
01	10	10	10	[illegible]	[illegible]	[illegible]	[illegible]	[illegible]	[illegible]	[illegible]	[illegible]	10	[illegible]	[illegible]	10	10	10
				10	10	10	10	10	10	10	10	10	10	10	10	10	10
02	10	10	10	10	10	10	10	10	10	10	10	10	10	10	10	10	10
				10	10	10	10	10	10	10	10	10	10	10	10	10	10
03	10	10	10	10	10	10	10	10	10	10	10	10	10	10	10	10	10
				[illegible]	[illegible]	[illegible]	[illegible]	[illegible]	[illegible]	[illegible]	[illegible]	[illegible]	[illegible]	[illegible]	[illegible]	10	10
04	10	10	10	[illegible]	[illegible]	[illegible]	[illegible]	[illegible]	[illegible]	[illegible]	[illegible]	10	10	10	10	10	10
				[illegible]	[illegible]	[illegible]	[illegible]	[illegible]	[illegible]	[illegible]	[illegible]	[illegible]	[illegible]	[illegible]	[illegible]	10	10
05	10	10	10	[illegible]	[illegible]	[illegible]	[illegible]	[illegible]	[illegible]	[illegible]	[illegible]	[illegible]	10	[illegible]	[illegible]	10	10
				[illegible]	[illegible]	[illegible]	[illegible]	[illegible]	[illegible]	[illegible]	[illegible]	[illegible]	[illegible]	[illegible]	10	10	10
53	10	10	10	10	10	10	10	10	10	10	10	10	10	10	10	10	10
				10	10	10	10	10	10	10	10	10	10	10	10	10	10
59	10	10	10	10	10	10	10	10	10	10	10	10	10	10	10	10	10
				11	10	[illegible]	[illegible]	[illegible]	[illegible]	[illegible]	[illegible]	[illegible]	[illegible]	[illegible]	[illegible]	10	10
60	10	10	10	[illegible]	[illegible]	[illegible]	[illegible]	[illegible]	[illegible]	[illegible]	[illegible]	[illegible]	[illegible]	[illegible]	10	10	10
				[illegible]	[illegible]	[illegible]	[illegible]	[illegible]	[illegible]	[illegible]	[illegible]	[illegible]	10	10	10	10	10
61	10	10	10	10	11	10	11	11	10	10	10	10	10	11	10	10	11
				11	12	10	10	10	10	10	10	10	10	10	10	10	10

Fig. 27. - C_k at 180 minutes, radiation B.C.

W AT H -FIELD IN MM / SEC STEP 180

I:	01	02	03	04/31	05/30	06/29	07/28	08/27	09/26	10/25	11/24	12/23	13/22	14/21	15/20	16/19	17/18
01	0	0	0	0	0	0	0	0	0	0	0	0	0	0	0	0	0
02	0	4	3	3	3	3	3	3	3	3	3	3	3	3	3	3	3
03	0	2	1	0	0	0	0	0	0	0	0	0	0	0	0	0	0
				0	-1	1	1	0	0	0	0	0	0	0	0	0	0
04	0	1	0	0	0	0	0	0	0	0	0	0	0	0	0	0	0
					-1												
58	0	2	0	0	0	0	0	0	0	0	0	0	0	0	0	0	0
				0	-1	1	0	0	0	0	0	0	0	0	0	0	0
59	0	2	1	1	1	1	1	1	1	1	1	1	1	1	1	1	1
60	0	-1	-2	[illegible]	[illegible]	[illegible]	[illegible]	-2	-2	-2	-2	-2	-2	-2	-2	-2	-2
61	0	0	0	0	0	0	0	0	0	0	0	0	0	0	0	0	0

05 97139 97797 פנטום בע״מ, שדרות טל

Fig. 28. – W_h at 180 minutes, constant B.C.

W AT H -FIELD IN MM / SEC STEP 180

I:	01	02	03	04/31	05/30	06/29	07/28	08/27	09/26	10/25	11/24	12/23	13/22	14/21	15/20	16/19	17/18
01	0	0	0	0	0	0	0	0	0	0	0	0	0	0	0	0	0
02	0	0	0	0	0	0	0	0	0	0	0	0	0	0	0	0	0
03	0	0	0	0	0	0	0	0	0	0	0	0	0	0	0	0	0
04	0	0	0	0	0	0	0	0	0	0	0	0	0	0	0	0	0
58	0	0	0	0	0	0	0	0	0	0	0	0	0	0	0	0	0
				0	0	0	0	0	0	0	0	0	0	0	0	0	0
59	0	0	0	0	0	0	0	0	0	0	0	0	0	0	0	0	0
60	0	-1	-1	0	0	0	0	0	0	0	0	0	0	0	0	0	0
61	0	0	0	0	0	0	0	0	0	0	0	0	0	0	0	0	0

05 97139 97797 פנטום בע״מ, שדרות טל

Fig. 29. – W_h at 180 minutes, radiation B.C.